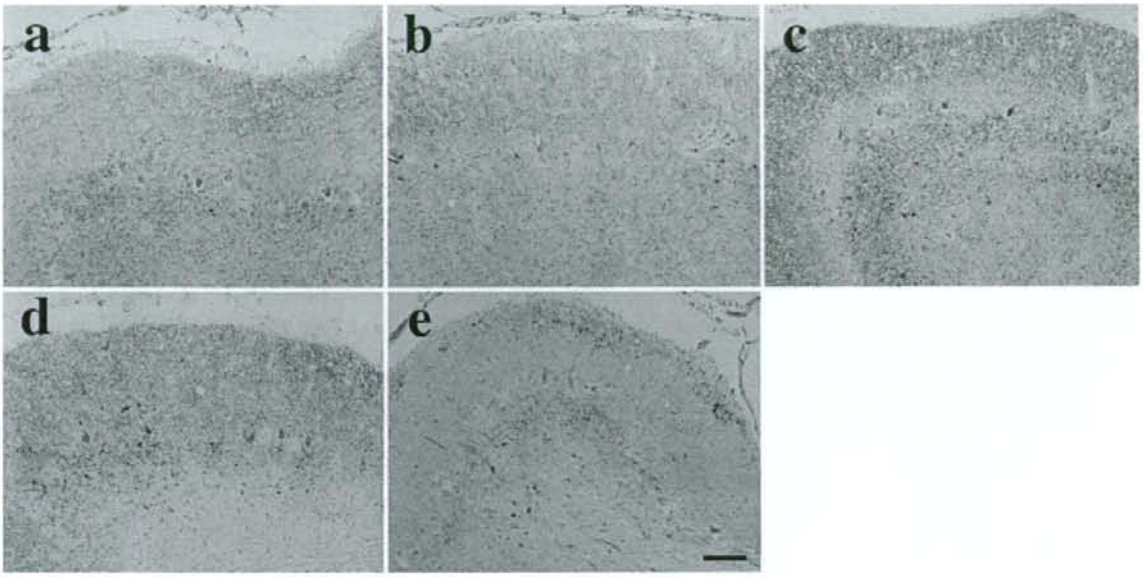

Fig. 6 PrP deposition in the cerebellar cortex in five dura mater-associated Creutzfeldt-Jakob disease (dura-CJD) cases. (a–d) Synaptic-type PrP deposition is present, particularly in the molecular and granule cell layers, in all cases. (e) PrP deposition is sparse in severe lesions. Some small-plaque-like PrP deposition is observed in the molecular and granule cell layers. (a) Case 1; (b) Case 2; (c) Case 3; (d) Case 4; (e) Case 5. PrP immunostaining. Scale bar = 100 μm.

peripherally infected mice.[32] Although it has been reported that cerebellar symptoms do not necessarily correlate with the anatomic site of grafting,[3] initial manifestations and/or EEG findings have been reported to be correlated with the graft site in some cases of dura-CJD.[12,15,21] In addition, initial symptoms of dura-CJD have been associated with MRI abnormalities of the dura mater graft sites.[30] In the present study, the symptoms of onset in four patients who received transplants below the cerebellar tent reflected cerebellar or brainstem involvement, and those in one patient who received transplant above the cerebellar tent reflected cerebral cortical involvement. According to these findings, we suggest that the infectious agent gains direct access to the brain surface from the graft. In the present study, a dura mater graft was used for a cervical lesion in one case, suggesting that transmission from contaminated dura mater grafts can occur in areas of the neuraxis outside of the cranial vault. Determination of the relation between clinical signs of onset and pathologic findings of the site of dura mater graft was an important objective of the present study; however, no apparent relation was identified. Diffusion-weighted MRIs could not be obtained for any of the present cases.

There was no evidence of particular accentuation of neuropathologic findings or PrP accumulation near the dura mater graft sites; synaptic-type PrP deposition was observed diffusely and symmetrically in the cerebrum,

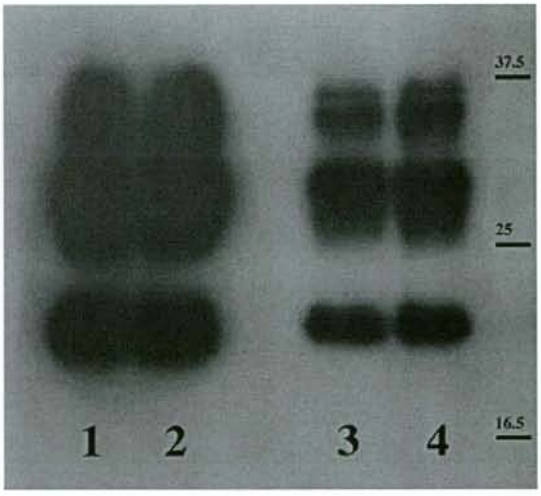

Fig. 7 Western blot analysis of protease-resistant Pr). The gel mobility of PrP from frozen frontal cerebral cortex of two of the present dura mater-associated Creutzfeldt-Jakob disease (dura-CJD) patients (lanes 2 and 3) are compared with that of two patients with MM1-type sporadic CJD (lanes 1 and 4). Lanes 2 and 3 correspond to cases 3 and 4, respectively, in the present study. Lanes 1 and 4 correspond to cases 9 and 11 in our previous report.[27] PrP migrated as three bands that have been shown to correspond to the diglycosylated (upper band), monoglycosylated (middle band) and non-glycosylated (lowest band) forms of the protein. The PrP glycoform ratios in the two dura-CJD patients are similar to that of MM1-type sporadic CJD.

cerebellum and brainstem in the present study. We believe that neuropathologic involvement and abnormal PrP accumulation must progress extensively by the time of autopsy. Our neuropathologic observations of dura-CJD were essentially the same as those of MM1- and MV1-type sporadic CJD reported by our laboratory[27,33,34] and by Parchi *et al.* [28] However, severity varied according to disease duration. In the present study, one case was classified as SSE, and four were classified as PE-type CJD. In the four PE-type CJD cases, the cerebral white matter showed myelin pallor with tissue rarefaction, numerous foamy macrophages and hypertrophic astrocytosis. Cerebral white matter lesions are considered rare in sporadic CJD in North America and Europe.[35] However, PE-type sporadic CJD is relatively common in Japan.[27] We have suggested that the pathologic difference between SSE and PE-type sporadic CJD is due mainly to disease duration.[27] We suggest the same for dura-CJD pathology. In Japan, most CJD patients, including dura-CJD patients, at the stage of akinetic mutism are managed carefully with supportive therapies until death. White matter lesions have been reported in some cases of dura-CJD.[10,20,21] In these cases, CJD disease duration was generally long (16 months, 10 months and 27 months, respectively).

Although dura-CJD is clinicopathologically similar to sporadic CJD,[20] another type of dura-CJD, characterized by the presence of florid plaques (plaque-type dura-CJD), has been reported.[7–10,14,17–19] In the present study, although synaptic-type PrP deposition was observed in all of the cases, kuru plaques or florid plaques were not observed (thus these cases were non-plaque-type dura-CJD). Patients with plaque-type dura-CJD show clinicopathologic features that are distinct from those of non-plaque-type dura-CJD and that resemble those of variant CJD cases; that is, a slow progressive clinical course with the absence or late occurrence of PSWCs on EEG and the presence of widespread florid plaques.[7–10,14,17–19] The reported disease duration of atypical dura-CJD with plaques is relatively prolonged (5–24 months),[7–10,14,17–19,36] similar to that of variant CJD (8–38 months).[37] Noguchi-Shinohara *et al.*[36] reported in an analysis of 23 Japanese patients with pathologically confirmed dura-CJD that the frequency of the plaque-type was 48%. However, they speculated that because plaque-type dura-CJD is associated with atypical features, these cases may be autopsied more frequently than non-plaque-type cases with classical CJD features (i.e., there may be a selection bias for autopsy).[36]

Variations in the clinicopathologic phenotype of CJD occur in response to disease duration, PrP genotype, including polymorphisms and mutations, and PrP strain.[2,27,28,35] Different PrP strains can be distinguished by disease characteristics in inbred animals.[2] Sporadic CJD has been classified into six subtypes according to the three genotypes of methionine (M)/valine (V) polymorphism at codon 129 of the PrP gene (MM, MV and VV) and two types of protease-resistant PrP (types 1 and 2).[28] Methionine homozygosity or valine homozygosity at codon 129 confers a genetic predisposition to sporadic CJD,[38] and heterozygosity at codon 129 may provide partial protection against sporadic as well as acquired CJD.[1,2] Susceptibility to prion infection is influenced significantly by the PrP gene codon 129 polymorphism.[1,2,39] For example, in cases of iatrogenic CJD from contaminated human growth hormone extracts, 50% were Val/Val, 31% were Met/Met and 19% were Met/Val.[1,2] All variant CJD cases tested have been methionine homozygotes.[2,3] In the present study, the three dura-CJD cases analyzed showed methionine homozygosity at codon 129. The majority of dura-CJD cases for which codon 129 polymorphism was examined showed methionine homozygosity.[7,8,13,14,16–21,29] However, Brown *et al.*[4] reported dura-CJD cases with MV or VV polymorphisms. Noguchi-Shinohara *et al.*[36] reported a pathologically unconfirmed dura-CJD patient in Japan with MV polymorphism at codon 129. The Japanese population shows 91.6% methionine homozygosity, 8.4% valine heterozygosity and 0% valine homozygosity.[40] We hypothesize that these percentages of codon 129 polymorphism, in addition to the widespread use of Lyodura, may indicate why many cases of dura-CJD occur in Japan.

Western blot analysis of protease-resistant PrP showed type 1 PrP in the two cases analyzed in the present study. We analyzed PrP type in one frozen cerebral cortex sample in each case. Thus, the possibility of the coexistence of type 1 and type 2 PrP in the present cases cannot be ruled out. However, we believe these patients should be classified as MM1-type CJD because all cases of dura-CJD without florid plaques in which PrP type has been examined have shown type 1 PrP.[15,20,29,36] Some cases with florid plaques have shown type 1 PrP,[7,14,17,19] and some clinically atypical dura-CJD cases with type 1 PrP have shown both synaptic- and plaque-type PrP deposits.[7,17]

In conclusion, no apparent clinicopathologic differences were found between dura-CJD cases in the present study and typical sporadic CJD cases, except for history of dura mater transplantation. Although a specific association between the dura mater graft site and neuropathologic observations was not evaluated in the present study, the initial symptoms appear to be closely related to the graft site, indicating a direct transmission of CJD from the graft site to the adjacent brain.

REFERENCES

1. DeArmond SJ, Dickson DW, DeArmond B. Human prion disease: degenerative disease of the central

nervous system. In: Davis RL, Robertson DM, eds. *A Textbook of Neuropathology*, 3rd edn. Baltimore: Williams & Wilkins, 1997; 1111–1125.
2. DeArmond SJ, Kretzschmar HA, Prusiner SB. Prion diseases. In: Graham DI, Lantos PL, eds. *Greenfield's Neuropathology*, Vol. 2, 7th edn. London: Hodder Arnold, 2002; 273–324.
3. Will RG. Acquired prion disease: iatrogenic CJD, variant CJD, kuru. *Br Med Bull* 2003; **66**: 255–265.
4. Brown P, Preece M, Brandel JP *et al.* Iatrogenic Creutzfeldt-Jakob disease at the millennium. *Neurology* 2000; **55**: 1075–1081.
5. Centers for Disease Control (CDC). Rapidly progressive dementia in a patient who received a cadaveric dura mater graft. *MMWR Morb Mortal Wkly Rep* 1987; **36**: 49–50, 55.
6. Centers for Disease Control and Prevention (CDC). Creutzfeldt-Jakob disease in patients who received a cadaveric dura mater graft – Spain, 1985–1992. *MMWR Morb Mortal Wkly Rep* 1993; **42**: 560–563.
7. Kimura K, Nonaka A, Tashiro H *et al.* Atypical form of dural graft associated Creutzfeldt-Jakob disease: report of a postmortem case with review of the literature. *J Neurol Neurosurg Psychiatry* 2001; **70**: 696–699.
8. Kopp N, Streichenberger N, Deslys JP, Laplanche JL, Chazot G. Creutzfeldt-Jakob disease in a 52-year-old woman with florid plaques. *Lancet* 1996; **348**: 1239–1240.
9. Kretzschmar HA, Sethi S, Földvári Z *et al.* Iatrogenic Creutzfeldt-Jakob disease with florid plaques. *Brain Pathol* 2003; **13**: 245–249.
10. Lane KL, Brown P, Howell DN *et al.* Creutzfeldt-Jakob disease in a pregnant woman with an implanted dura mater graft. *Neurosurgery* 1994; **34**: 737–739.
11. Lang CJ, Schuler P, Engelhardt A, Brown P. Probable Creutzfeldt-Jakob disease after a cadaveric dural graft. *Eur J Epidemiol* 1995; **11**: 79–81.
12. Masullo C, Pocchiari M, Macchi G, Alema G, Piazza G, Panzera MA. Transmission of Creutzfeldt-Jakob disease by dural cadaveric graft. *J Neurosurg* 1989; **71**: 954–955.
13. Miyashita K, Inuzuka T, Kondo H *et al.* Creutzfeldt-Jakob disease in a patient with a cadaveric dural graft. *Neurology* 1991; **41**: 940–941.
14. Mochizuki Y, Mizutani T, Tajiri N *et al.* Creutzfeldt-Jakob disease with florid plaques after cadaveric dura mater graft. *Neuropathology* 2003; **23**: 136–140.
15. Nishida Y, Yamada M, Hara K *et al.* Creutzfeldt-Jakob disease after Jannetta's operation with cadaveric dura mater graft: initial manifestations related to the grafted site. *J Neurol* 2002; **249**: 480–483.
16. Preusser M, Strobel T, Gelpi E *et al.* Alzheimer-type neuropathology in a 28 year old patient with iatrogenic Creutzfeldt-Jakob disease after dural grafting. *J Neurol Neurosurg Psychiatry* 2006; **77**: 413–416.
17. Shimizu S, Hoshi K, Muramoto T *et al.* Creutzfeldt-Jakob disease with florid-type plaques after cadaveric dura mater grafting. *Arch Neurol* 1999; **56**: 357–362.
18. Takashima S, Tateishi J, Taguchi Y, Inoue H. Creutzfeldt-Jakob disease with florid plaques after cadaveric dural graft in a Japanese woman. *Lancet* 1997; **350**: 865–866.
19. Wakisaka Y, Santa N, Doh-ura K *et al.* Increased asymmetric pulvinar magnetic resonance imaging signals in Creutzfeldt-Jakob disease with florid plaques following a cadaveric dura mater graft. *Neuropathology* 2006; **26**: 82–88.
20. Yamada M, Itoh Y, Suematsu N, Matsushita M, Otomo E. Panencephalopathic type of Creutzfeldt-Jakob disease associated with cadaveric dura mater graft. *J Neurol Neurosurg Psychiatry* 1997; **63**: 524–527.
21. Yamada S, Aiba T, Endo Y, Hara M, Kitamoto T, Tateishi J. Creutzfeldt-Jakob disease transmitted by a cadaveric dura mater graft. *Neurosurgery* 1994; **34**: 740–743.
22. Brown P, Brandel JP, Preece M, Sato T. Iatrogenic Creutzfeldt-Jakob disease: the waning of an era. *Neurology* 2006; **67**: 389–393.
23. Centers for Disease Control and Prevention (CDC). Creutzfeldt-Jakob disease associated with cadaveric dura mater grafts – Japan, January 1979–May 1996. *MMWR Morb Mortal Wkly Rep* 1997; **46**: 1066–1069.
24. Centers for Disease Control and Prevention (CDC). Update: Creutzfeldt-Jakob disease associated with cadaveric dura mater grafts – Japan, 1979–2003. *MMWR Morb Mortal Wkly Rep* 2003; **52**: 1179–1181.
25. Hoshi K, Yoshino H, Urata J, Nakamura Y, Yanagawa H, Sato T. Creutzfeldt-Jakob disease associated with cadaveric dura mater grafts in Japan. *Neurology* 2000; **55**: 718–721.
26. Kascsak RJ, Rubenstein R, Merz PA *et al.* Mouse polyclonal and monoclonal antibody to scrapie-associated fibril proteins. *J Virol* 1987; **61**: 3688–3693.
27. Iwasaki Y, Yoshida M, Hashizume Y, Kitamoto T, Sobue G. Clinicopathologic characteristics of sporadic Japanese Creutzfeldt-Jakob disease classified according to prion protein gene polymorphism and prion protein type. *Acta Neuropathol (Berl)* 2006; **112**: 561–571.
28. Parchi P, Giese A, Capellari S *et al.* Classification of sporadic Creutzfeldt-Jakob disease based on molecular and phenotypic analysis of 300 subjects. *Ann Neurol* 1999; **46**: 224–233.
29. Satoh K, Muramoto T, Tanaka T *et al.* Association of an 11–12 kDa protease-resistant prion protein fragment with subtypes of dura graft-associated

Creutzfeldt-Jakob disease and other prion diseases. *J Gen Virol* 2003; **84**: 2885–2893.
30. Sato T, Masuda M, Utsumi Y *et al.* Dura mater related Creutzfeldt-Jakob disease in Japan: relationship between sites of grafts and initial clinical features. In: Kitamoto T, ed. *Prions: Food and Drug Safety*. Tokyo: Springer-Verlag, 2005; 31–40.
31. Kimberlin RH. Transmissible encephalopathies in animals. *Can J Vet Res* 1990; **54**: 30–37.
32. McBride PA, Bruce ME, Fraser H. Immunostaining of scrapie cerebral amyloid plaques with antisera raised to scrapie-associated fibrils (SAF). *Neuropathol Appl Neurobiol* 1988; **14**: 325–336.
33. Iwasaki Y, Hashizume Y, Yoshida M, Kitamoto T, Sobue G. Neuropathologic characteristics of brainstem lesions in sporadic Creutzfeldt-Jakob disease. *Acta Neuropathol (Berl)* 2005; **109**: 557–566.
34. Iwasaki Y, Yoshida M, Hashizume Y, Kitamoto T, Sobue G. Neuropathologic characteristics of spinal cord lesions in sporadic Creutzfeldt-Jakob disease. *Acta Neuropathol (Berl)* 2005; **110**: 490–500.
35. Budka H, Aguzzi A, Brown P *et al.* Neuropathological diagnostic criteria for Creutzfeldt-Jakob disease (CJD) and other human spongiform encephalopathies (prion diseases). *Brain Pathol* 1995; **5**: 459–466.
36. Noguchi-Shinohara M, Hamaguchi T, Kitamoto T. *et al.* Clinical features and diagnosis of dura mater graft-associated Creutzfeldt-Jakob disease. *Neurology* 2007; **69**: 360–367.
37. Will RG, Zeidler M, Stewart GE *et al.* Diagnosis of new variant Creutzfeldt-Jakob disease. *Ann Neurol* 2000; **47**: 575–582.
38. Palmer MS, Dryden AJ, Hughes JT, Collinge J. Homozygous prion protein genotype predisposes to sporadic Creutzfeldt-Jakob disease. *Nature* 1991; **352**: 340–342.
39. Collinge J, Palmer MS, Dryden AJ. Genetic predisposition to iatrogenic Creutzfeldt-Jakob disease. *Lancet* 1991; **337**: 1441–1442.
40. Doh-ura K, Kitamoto T, Sakaki Y, Tateishi J. CJD discrepancy. *Nature* 1991; **353**: 801–802.

Neuropathology 2008; **28**, 326–332 doi:10.1111/j.1440-1789.2007.00854.x

Case Report

MM1-type sporadic Creutzfeldt-Jakob disease with unusually prolonged disease duration presenting with panencephalopathic-type pathology

Akira Hoshino,[1] Yasushi Iwasaki,[2] Masayuki Izumi,[1] Shinya Kimura,[3] Tohru Ibi,[1] Tetsuyuki Kitamoto,[4] Mari Yoshida,[5] Yoshio Hashizume[5] and Ko Sahashi[1]

[1]Department of Neurology, Aichi Medical University School of Medicine, Aichi, [2]Department of Neurology, Nagoya University Graduate School of Medicine, Nagoya, [3]Department of Rehabilitation Medicine, Aichi Medical University School of Medicine, Aichi, [4]Division of CJD Science and Technology, Department of Prion Research, Center for Translational and Advanced Animal Research on Human Diseases, Tohoku University Graduate School of Medicine, Sendai, and [5]Department of Neuropathology, Institute for Medical Science of Aging, Aichi Medical University, Aichi, Japan

We report an autopsy case of MM1-type sporadic Creutzfeldt-Jakob disease (sCJD) with an unusually prolonged disease duration of 58 months. The initial symptom was progressive mental disorder followed by advanced cognitive impairment. Clinical progression was generally slow; myoclonus appeared at 17 months and periodic sharp-wave complexes on electroencephalogram at 21 months. A state of akinetic mutism occurred 29 months after the onset of symptoms. MRI showed gradually progressive cerebral atrophy. Neuropathologic examination showed widespread severe brain involvement. In the cerebral neocortex, widespread severe tissue rarefaction, hypertrophic astrocytosis and neuron loss (so-called status spongiosus) were observed. The cerebral white matter showed diffuse myelin pallor with intense hypertrophic astrocytosis, numerous foamy macrophages and emperipolesis, indicating panencephalopathic-type sCJD pathology. The brainstem was relatively preserved from sCJD pathology, with the exception of the pontine nucleus and pyramidal tract. This may explain the prolonged disease duration without respiratory insufficiency until the terminal stage. Immunohistochemistry for prion protein (PrP) showed widespread synaptic-type PrP deposits in the cerebral neocortex, hippocampus and thalamus. The striatum and cerebellar cortex showed faint synaptic-type PrP deposition with some areas of small plaque-like PrP deposition. Sparse PrP deposition was also observed in the brainstem. Analysis of the PrP gene showed no mutation but methionine homozygosity at polymorphic codon 129. Western blot analysis of protease-resistant PrP indicated type 1 PrP. To our knowledge, this is the longest reported disease duration of MM1-type sCJD.

Key words: MM1-type, panencephalopathic-type, prolonged disease duration, sporadic Creutzfeldt-Jakob disease, status spongiosus.

INTRODUCTION

The clinicopathologic presentation of sporadic Creutzfeldt-Jakob disease (sCJD) is influenced by several factors, including the prion strain and polymorphism of the prion protein (PrP) gene of the host.[1–3] Analyses of neuropathologic findings as well as of clinical features will provide a better understanding of such factors.[1–3] On the basis of their comprehensive analysis of molecular and clinicopathologic features of a large series of sCJD patients, Parchi *et al.*[3] proposed classification of sCJD into six distinct subgroups (MM1, MM2, MV1, MV2, VV1 and VV2). Although such classification is helpful in the identification and understanding of major disease subgroups, there remain individual cases that prove difficult to classify.[4–6] Usually, MM1- and MV1-type sCJD include cases previously classified as typical sCJD of the myoclonic type or as Heidenhain variant and show the most common characteristics of sCJD, including rapidly progressive myoclonic dementia associated with periodic sharp-

Correspondence: Yasushi Iwasaki, MD, Department of Neurology, Nagoya University Graduate School of Medicine, 65 Tsurumai-cho, Showa-ku, Nagoya 466-8550, Japan. Email: iwasaki@sc4.so-net.ne.jp
Received 12 June 2007; revised and accepted 2 August 2007.

wavecomplexes (PSWCs) on electroencephalogram (EEG).[2,3]

We performed a postmortem examination of a patient with MM1-type sCJD with a 58-month history of slowly progressive mental disorder and cognitive impairment with PSWCs and myoclonus. To our knowledge, this is the longest reported disease duration of MM1-type sCJD. The neuropathologic findings of the present case appear to reflect the terminal pathology of MM1-type sCJD. Interestingly, the present patient also showed an unusually slow progression of the disease. We describe the clinicopathologic findings and discuss aspects of this case with respect to sCJD phenotypic variability. This patient corresponds to patient No. 20 and patient No. 10 in our previous reports, respectively.[2,7]

CLINICAL SUMMARY

A 53-year-old Japanese woman living in the Aichi prefecture showed behavioral changes starting in December 1997. Three months later, the patient showed loss of balance, and involuntary movements around the mouth appeared. Depression, anxiety, confusion and abnormal behavior were observed, and she was admitted to the Department of Neurology at Aichi Medical University School of Medicine in August 1998. The patient had no history of surgery or known iatrogenic exposure to CJD or any family history of prion disease. Neurologic examination showed memory disturbance, intellectual decline, emotional imbalance and oral dyskinesia, but dysarthria and bulbar palsy were not apparent at this stage. Her gait was wide-based with truncal ataxia, and deep tendon reflexes in the extremities were slightly exaggerated, with a positive Babinski sign on the right side. Superficial sensations were not affected. MRI was performed in October 1998 and showed no brain atrophy, and EEG revealed normal activity without PSWCs. MR diffusion-weighted images were not available. Lumbar puncture was performed; CSF contained 71 mg glucose/dL and 35 mg protein/dL, with 1 lymphocyte/mm^3. CSF 14-3-3 protein was not examined. Mental disorder, including depression, anxiety and confusion, became more apparent. By November 1998, gait disturbance had progressed, and the patient had difficulty walking. Dysarthria was observed at this stage, and the patient occasionally used meaningless words. A generalized convulsion-like episode occurred in December 1998. By March 1999, dysphagia, involuntary movements of the extremities and nystagmus had appeared, and conversation had become impossible. She suffered aspiration pneumonia and intermittent generalized convulsions in April 1999. In May 1999, although the pneumonia had been slowly improving, myoclonus was observed. Tracheotomy was performed due to severe dysphagia. CT of the brain in September 1999 showed severe cerebral atrophy, and PSWCs were observed. Myoclonus disappeared in November 1999. Oral dyskinesia and nystagmus gradually disappeared, and the patient entered a state of akinetic mutism 29 months after the onset of symptoms. EEG showed generalized slow-wave activity without PSWCs at this stage. In June 2000, maintenance of body temperature became difficult, probably due to dysautonomia, and a urinary catheter was inserted. MRI showed marked cerebral, cerebellar and brainstem atrophy in September 2000 (Fig. 1). In January 2001, the anal sphincter muscles showed persistent relaxation, and the cough reflex disappeared. The patient was fed by nasogastric tube and treated with antibiotics for bronchopneumonia and urinary inflammation until death. Skin symptoms, such as pemphigoid, appeared in April 2002. On October 4, 2002, she experienced sudden respiratory insufficiency and died 58 months after the onset of symptoms. Respiration was preserved without any assistance until death.

Fig. 1 T1-weighted MRIs, obtained 26 months prior to death, show severe cerebral, cerebellar and brainstem atrophy. R, right side.

METHODS

Neuropathologic examination

The brain was fixed in 20% neutral-buffered formalin, tissue blocks were cut and immersed in 95% formic acid (Wako Pure Chemical Industries, Osaka, Japan) for 2 h to inactivate PrP and paraffin-embedded sections were prepared. For routine neuropathologic examination, sections were subjected to HE and Klüver-Barrera staining.

Immunohistochemical analysis of selected sections was carried out with 3F4 anti-PrP mouse monoclonal antibody (1:100; Dako, Glostrup, Denmark) after antigen retrieval by hydrolytic autoclaving.[8] The PrP immunostaining protocol was as described previously.[9] Peroxidase-conjugated streptavidin was visualized with 3,3′-diaminobenzidine

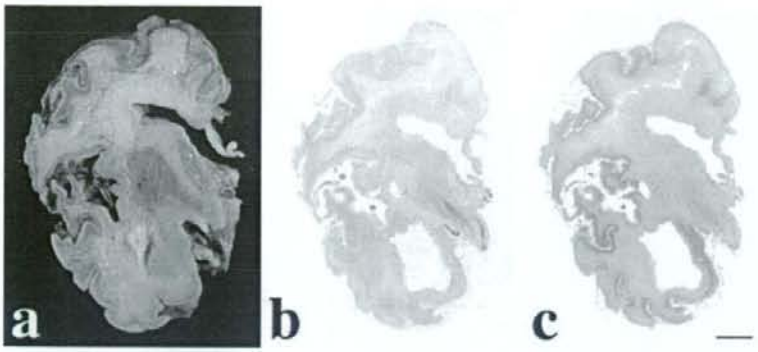

Fig. 2 Macroscopic appearance of coronal sections of cerebral hemisphere. (a) Severe cerebral neocortical atrophy is observed, and the lateral ventricles are severely enlarged. The striatum and thalamus show brownish atrophy. The cerebral white matter is soft and shows severe loss of volume. (b) The cerebral white matter shows severe myelin pallor. U-fibers are relatively preserved from myelin loss. Klüver-Barrera staining. (c) Immunostaining for prion protein (PrP) shows PrP staining mainly in the cerebral neocortex, hippocampus and basal ganglia. Scale bar, 10 mm.

Fig. 3 Macroscopic appearance of sagittal sections of cerebellar hemisphere. (a) Cerebellar cortical and white matter atrophy are apparent. (b) The cerebellar white matter shows severe myelin pallor. The dentate nucleus is relatively preserved. Klüver-Barrera staining. (c) Immunostaining for prion protein (PrP) shows widespread faint PrP staining in the cerebellar cortex. The dentate nucleus shows moderate PrP staining. Scale bar, 10 mm.

(Wako Pure Chemical Industries) as the final chromogen. All immunostained sections were lightly counterstained with Mayer's hematoxylin.

PrP gene analysis

An occipital lobe block, obtained at the time of autopsy, was cryopreserved at –80°C. Genomic DNA was extracted from the block and used to amplify the open reading frame of the PrP gene by PCR. We searched for PrP gene mutations and polymorphisms at codons 129 and 219 by restriction fragment length polymorphism analysis and by sequencing, as described previously.[2]

Western blot analysis of PrP

A sample of cryopreserved cerebral cortex was homogenized, and Western blot analysis of protease-resistant PrP was performed with monoclonal antibody 3F4, as described previously.[2] Typing of PrP was performed on the basis of the classification system proposed by Parchi *et al.*[3]

PATHOLOGIC FINDINGS

Macroscopic findings

The brain weight was 800 g, and the cerebrum showed severe atrophy. Coronal sections of the cerebral hemisphere showed that the neocortex was very thin, and the ventricles were severely enlarged (Fig. 2a). Slight atrophy of the hippocampus and amygdala was observed. The striatum and thalamus showed brownish atrophy. The cerebral white matter was soft and showed severe loss of volume. The cerebellum and brainstem also showed severe atrophy (Figs 3a,4a).

Microscopic findings

In the cerebral neocortex, widespread severe tissue rarefaction, hypertrophic astrocytosis and neuron loss, so-called status spongiosus, were observed (Fig. 5a). Formations of marked cavitation were observed in some areas of severely affected neocortex (Fig. 5b). Medial portions of the temporal lobe, hippocampus and cingulate gyrus and the orbital surface of the frontal lobe were relatively preserved compared to the neocortex. Some ballooned neurons and atrophied neurons were identified in these preserved areas. Although typical spongiform changes were not readily identified, some areas of fine vacuole-type spongiform change (microvacuolar pattern with multiple single-rounded spaces within the neuropil[10,11]) were observed in the subiculum, area CA1-2 and the amygdala (Fig. 5c). In the striatum and thalamus, severe involvement similar to that of the neocortex was observed (Fig. 5d,e), whereas the nucleus of Meynert, amygdala and hypothalamus were relatively preserved. The cerebral white matter showed diffuse myelin pallor with intense hypertrophic

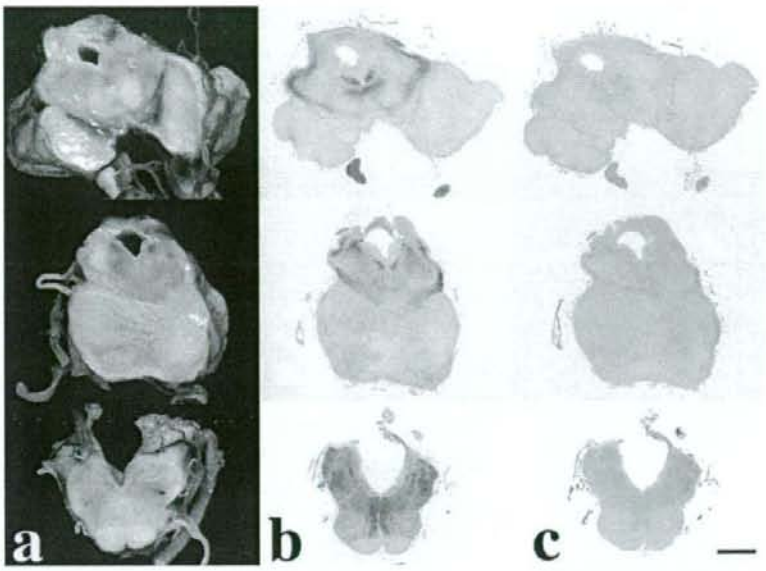

Fig. 4 Macroscopic appearance of horizontal sections of brainstem. (a) The midbrain shows slight tegmental atrophy. The pontine base shows severe atrophy, whereas the pontine tegmentum is well preserved. The medulla oblongata shows degeneration of the inferior olivary nucleus. (b) Severe loss of myelin is apparent in the tegmentum of the midbrain, cerebral peduncle, pontine base and pyramid of the medulla oblongata. The inferior olivary nucleus shows pseudohypertrophy. Klüver-Barrera staining. (c) Sparse to mild prion protein staining is observed in the quadrigeminal body, substantia nigra, pontine nucleus and inferior olivary nucleus. Scale bar, 5 mm.

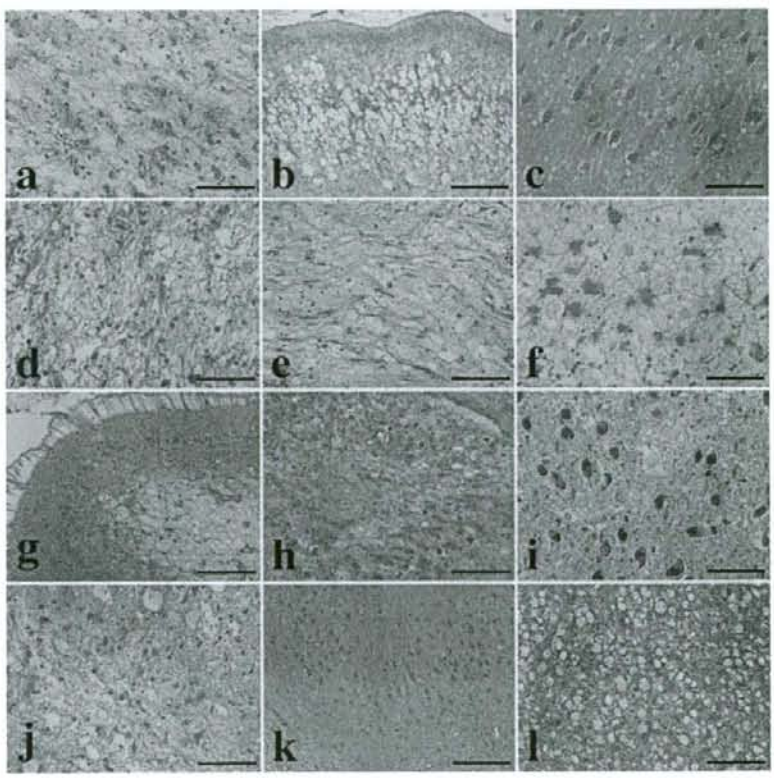

Fig. 5 Microscopic appearance of representative lesions. (a) The cerebral neocortex shows widespread status spongiosus with intense hypertrophic astrocytosis. Frontal lobe. (b) Formations of marked cavitation are observed in some severely affected neocortical lesions. The molecular layer is relatively preserved. (c) The hippocampus shows fine vacuole-type spongiform change without neuron loss. Area CA1. (d) The striatum also shows status spongiosus. Putamen. (e) The medial thalamus shows almost complete loss of neurons, tissue rarefaction and hypertrophic astrocytosis. Medial thalamic nucleus. (f) The cerebral white matter shows severe tissue rarefaction, numerous foamy macrophages and hypertrophic astrocytosis. Many instances of emperipolesis, in which hypertrophic astrocytes engulf one to several oligodendrocytes within their cytoplasm, are present. Frontal lobe. (g) The cerebellar cortex shows moderate loss of Purkinje neurons. Bergmann's gliosis and some torpedoes are observed. The molecular layer shows severe atrophy, and the granule cell layer shows severe neuron loss. (h) The dentate nucleus shows tissue rarefaction and gliosis but is relatively preserved from neuron loss. (i) The substantia nigra shows tissue rarefaction and gliosis without apparent loss of pigmented neurons. (j) The pontine nucleus shows severe neuron loss and hypertrophic astrocytosis. (k) The inferior olivary nucleus shows mild neuron loss and moderate hypertrophic astrocytosis. (l) Severe degeneration with hypertrophic astrocytosis and numerous foamy macrophages is observed in the pyramid of the medulla oblongata. HE staining. Scale bars: a, c, d, e, f, i, j, k, 100 μm; g, h, l, 200 μm; b, 0.5 mm.

astrocytosis, and numerous foamy macrophages were observed. These findings indicated panencephalopathic (PE)-type pathology (Fig. 2b).[2,10,12] Within the involved cerebral white matter, many instances of emperipolesis, in which hypertrophic astrocytes engulf one to several oligodendrocytes within their cytoplasm,[13] were observed (Fig. 5f). U-fibers were relatively preserved from myelin loss. In the optic nerve, myelin loss was also apparent, and many foamy macrophages were observed. In the cerebellum, the molecular layer showed severe atrophy, and the granule cell layer showed almost complete loss of neurons and many torpedoes; mild loss of Purkinje neurons and Bergmann's gliosis were observed (Fig. 5g). The dentate nucleus showed tissue rarefaction and gliosis but was relatively preserved from neuron loss (Fig. 5h). Loss of myelin and axons was remarkable in the cerebellar white matter (Fig. 3b). In the brainstem, severe loss of myelin was apparent in the tegmentum of the midbrain, cerebral peduncle, pontine base and pyramid of the medulla oblongata (Fig. 4b). The periaqueductal gray nuclei of the oculomotor nerve and trochlear nerve, locus ceruleus, superior central nucleus, motor nucleus of the trigeminal nerve, nucleus of the hypoglossal nerve and dorsal nucleus of the vagal nerve were relatively preserved from neuron loss, but mild to moderate gliosis was apparent. The substantia nigra showed tissue rarefaction and gliosis without apparent loss of pigmented neurons (Fig. 5i). Severe neuron loss with hypertrophic astrocytosis of the pontine nucleus was observed (Fig. 5j). Among the pontine transverse fibers, superior cerebellar peduncle and central tegmental tract, many foamy macrophages were observed. Medial longitudinal fibers and the lateral and medial lemnisci were relatively preserved from myelin and axon loss. The inferior olivary nucleus showed pseudohypertrophy, mild neuron loss and hypertrophic astrocytosis (Figs 4b,5k). Severe degeneration with loss of myelin and axons, hypertrophic astrocytosis and foamy macrophages were observed in the pyramidal tracts including the internal capsule, cerebral pedunculus of the midbrain, pontine longitudinal fibers and the pyramid of the medulla oblongata (Fig. 5l). Kuru plaques and florid plaques were not identified. No senile plaques, neurofibrillary tangles or Lewy bodies were found.

PrP immunohistochemical findings

Synaptic-type PrP deposition, indicated by diffuse positive granular staining, was observed in the cerebral neocortex but was generally faint (Figs 2c,6a). PrP deposition was more apparent in relatively preserved areas including the hippocampus, subiculum, amygdala, cingulate gyrus, orbital surface of the frontal lobe, internal segment of the globus pallidus, rostral portion of the parahippocampal gyrus and cerebellar dentate nucleus (Figs 3c,6b). The striatum and cerebellar cortex showed weak synaptic-type PrP deposition with some areas of small plaque-like PrP deposition (Fig. 3c,6c,d). Weak PrP deposition was observed in the thalamus, tegmentum of the brainstem, substantia nigra and inferior olivary nucleus (Fig. 4c). In the pontine nucleus, PrP deposition was very sparse. No definitive PrP staining was identified in the cerebral or cerebellar white matter.

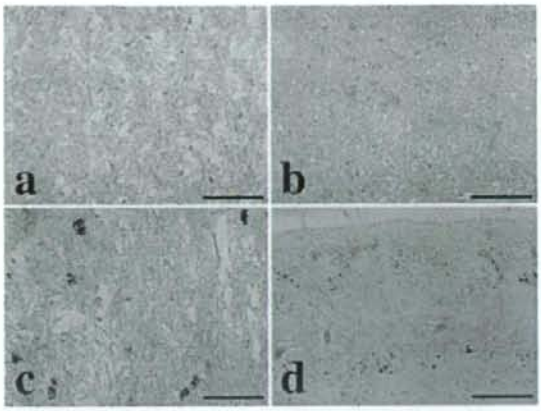

Fig. 6 Microscopic appearance of representative lesions by prion protein (PrP) immunostaining. (a) The cerebral neocortex shows widespread synaptic-type PrP deposition. Temporal lobe. (b) The hippocampus shows moderate synaptic-type PrP deposition. Subiculum. (c) The basal ganglia show moderate synaptic-type PrP deposition with some areas of small plaque-like PrP deposition. Putamen. (d) The cerebellar cortex shows faint synaptic-type deposition with areas of small plaque-like PrP deposition in the molecular and granule cell layers. PrP immunostaining. Scale bars, 100 μm.

PrP gene analysis and Western blot analysis

No mutation of the PrP gene open reading frame was identified, and methionine homozygosity at codon 129 was determined. Codon 219 showed glutamic acid homozygosity. Western blot analysis disclosed a type 1 three-band pattern, with the relative molecular mass of the non-glycosylated band being 21 kDa. Accordingly, this case was classified as MM1-type sCJD.[3]

DISCUSSION

Neuropathologic hallmarks of sCJD include spongiform change in the neuropil, neuron loss, intense hypertrophic astrocytosis and deposition of abnormal protease-resistant PrP.[2,10,14] In patients with MM1-type sCJD, variable degrees of neuropathologic involvement are observed in the cerebral neocortex, subiculum, striatum, thalamus and cerebellar cortex, whereas the globus pallidus, hippocampus and dentate gyrus, brainstem and spinal cord are relatively

spared.[2,3,10,11,14-16] We analyzed PrP type only in one frozen cerebral cortex sample in the present case. Thus, the possibility of the coexistence of type 1 and type 2 PrP in the present case cannot be ruled out. However, we believe this patient should be classified as MM1-type sCJD for the following reasons: large confluent vacuole-type spongiform change and perivacuolar-type PrP deposition, which are characteristic of MM2-cortical-type sCJD,[2,3] were not observed in the cerebral cortices, and particular inferior olivary degeneration, which is found in MM2-thalamic-type sCJD,[2,3] was not observed. Our previous neuropathologic observations of Japanese MM1- and MV1-type sCJD cases[2] were similar to those of Parchi *et al.*[3] although the neuropathologic severity varied according to disease duration.[2] The present case showed widespread severe brain involvement, including the cerebral and cerebellar white matter, and showed terminal sCJD pathology such as that observed in the burnt-out stage.[10] Interestingly, the brainstem was relatively preserved, with the exception of the pontine nucleus and pyramidal tract; this may explain the prolonged disease duration without respiratory insufficiency until the terminal stage. We have reported that although the accumulation of PrP in the brainstem appears to be an early pathologic event in sCJD, the brainstem remains relatively resistant to the pathologic process of sCJD.[9,16] We have also suggested that subacute spongiform encephalopathy (SSE) and PE-type sCJD comprise the primary sCJD subtypes and that PE-type sCJD is a prolonged pathologic phenotype of SSE.[2,17] Japanese patients with sCJD have generally prolonged disease duration.[2,17] Therefore, we believe the Japanese population may include many cases of PE-type sCJD. We believe the reason Japanese patients with sCJD show prolonged disease duration is due to the intensive treatment of sCJD in Japan. Whether the clinical progression of PE-type sCJD is slower than that of SSE has not been clarified.

Clinical presentation of the present case included mental disorder (depression, anxiety, confusion and abnormal behavior), cognitive impairment (memory disturbance and intellectual decline), myoclonus and PSWCs, relatively common symptoms of MM1-type sCJD.[1-3] However, this case had an unusually prolonged disease duration of 58 months, and clinical progression was generally slow. For example, myoclonus did not appear until 17 months, PSWCs did not appear until 21 months and a state of akinetic mutism did not appear until 29 months after the onset of symptoms. In our autopsy series of sCJD including the present patient,[2] this patient was clearly distinguished from the other MM1-type sCJD cases as with respect to clinical presentation but not with respect to pathologic findings. No other MM1-type sCJD patients showed an intermediate clinical presentation between typical MM1-type sCJD and that of this patient. Parchi *et al.*[3] examined 300 cases of sCJD, and the most common subtype was MM1-type sCJD (67.7%), with a mean age at onset of 65.5 years (range, 42–91 years) and a mean disease duration of 3.9 months (range, 1–18 months). The mean times for the appearance of myoclonus and PSWCs were 1.8 and 2 months after onset, respectively.[3] According to the clinical presentation of the present case, we hypothesize that there may be a rare subtype of MM1-type sCJD with a slowly progressive disease course. Yamamoto *et al.*[6] reported a unique MM1-type sCJD case with a remarkably long clinical course of 50 months; PSWCs appeared at 13 months, a state of akinetic mutism appeared at 16 months and myoclonus appeared at 26 months after the onset of symptoms. MM1-type sCJD is viewed as a single entity by Parchi *et al.*[3] However, two other classifications proposed by Collinge *et al.*[18] and Zanusso *et al.*[19] divide MM1-type sCJD into two subtypes on the basis of different molecular masses of PrP and different phenotypic characteristics, primarily disease duration. Zanusso *et al.*[19] reported that one subtype of MM1-type sCJD shows different clinical presentation and significantly longer disease duration than are shown by other subtypes. However, Cali *et al.*[20] concluded that, with the exception of disease duration and duration-related neuropathologic findings, MM1-type sCJD patients with long and short disease duration showed no significant differences. Further detailed clinicopathologic study of MM1-type sCJD cases will be necessary to clarify this issue.

Intensive care of sCJD patients, even after the development of akinetic mutism, is common in Japan. The duration from the onset of symptoms to the development of akinetic mutism in Japanese patients (29 months in the present patient) largely corresponds to the total disease duration (58 months in the present patient) in Western countries. Neuropathologic findings in the present patient were not different from those in sCJD patients who live long after akinetic mutism appears.[2] Because this patient showed terminal CJD pathology, whether the pathologic findings were related to the slow progression of the disease could not be addressed.

In conclusion, the present case showed the longest disease duration of MM1-type sCJD yet reported, and the neuropathologic findings certainly reflect the terminal pathology of sCJD. Interestingly, the present case showed different patterns of slowly progressive clinical presentation than previously reported MM1-type sCJD cases. We hypothesize that there may be a rare subtype of MM1-type sCJD with a slowly progressive disease course. Identification of a novel subtype from the clinical phenotype of a single patient may be inappropriate. To determine whether MM1-type sCJD with a slowly progressive disease course represents a subtype or should be considered within the clinical spectrum of MM1-type sCJD will require further examination with a larger number of patients.

ACKNOWLEDGMENTS

This work was supported in part by the Research Grant (17A-10, KS) for Nervous and Mental Disorders from the Ministry of Health, Labour and Welfare of Japan.

REFERENCES

1. Gambetti P, Kong Q, Zou W, Parchi P, Chen SG. Sporadic and familial CJD: classification and characterisation. *Br Med Bull* 2003; **66**: 213–239.
2. Iwasaki Y, Yoshida M, Hashizume Y, Kitamoto T, Sobue G. Clinicopathologic characteristics of sporadic Japanese Creutzfeldt-Jakob disease classified according to prion protein gene polymorphism and prion protein type. *Acta Neuropathol (Berl)* 2006; **112**: 561–571.
3. Parchi P, Giese A, Capellari S *et al.* Classification of sporadic Creutzfeldt-Jakob disease based on molecular and phenotypic analysis of 300 subjects. *Ann Neurol* 1999; **46**: 224–233.
4. Hirose K, Iwasaki Y, Izumi M *et al.* MM2-thalamic-type sporadic Creutzfeldt-Jakob disease with widespread neocortical pathology. *Acta Neuropathol (Berl)* 2006; **112**: 503–511.
5. Ironside JW, Ritchie DL, Head MW. Phenotypic variability in human prion diseases. *Neuropathol Appl Neurobiol* 2005; **31**: 565–579.
6. Yamamoto S, Furukawa H, Kitamoto T *et al.* An atypical form of sporadic panencephalopathic Creutzfeldt-Jakob disease in Japan. *Neuropathol Appl Neurobiol* 2003; **29**: 77–80.
7. Iwasaki Y, Mimuro M, Yoshida M *et al.* Enhanced aquaporin-4 immunoreactivity in sporadic Creutzfeldt-Jakob disease. *Neuropathology* 2007; **27**: 314–323.
8. Kitamoto T, Shin RW, Doh-ura K *et al.* Abnormal isoform of prion proteins accumulates in the synaptic structures of the central nervous system in patients with Creutzfeldt-Jakob disease. *Am J Pathol* 1992; **140**: 1285–1294.
9. Iwasaki Y, Hashizume Y, Yoshida M, Kitamoto T, Sobue G. Neuropathologic characteristics of brainstem lesions in sporadic Creutzfeldt-Jakob disease. *Acta Neuropathol (Berl)* 2005; **109**: 557–566.
10. Budka H, Aguzzi A, Brown P *et al.* Neuropathological diagnostic criteria for Creutzfeldt-Jakob disease (CJD) and other human spongiform encephalopathies (prion diseases). *Brain Pathol* 1995; **5**: 459–466.
11. Kretzschmar HA, Ironside JW, DeArmond SJ, Tateishi J. Diagnostic criteria for sporadic Creutzfeldt-Jakob disease. *Arch Neurol* 1996; **53**: 913–920.
12. Mizutani T, Okumura A, Oda M, Shiraki H. Panencephalopathic type of Creutzfeldt-Jakob disease: primary involvement of the cerebral white matter. *J Neurol Neurosurg Psychiatry* 1981; **44**: 103–115.
13. Shintaku M, Yutani C. Oligodendrocytes within astrocytes ('emperipolesis') in the white matter in Creutzfeldt-Jakob disease. *Acta Neuropathol (Berl)* 2004; **108**: 201–206.
14. DeArmond SJ, Kretzschmar HA, Prusiner SB. Prion diseases. In: Graham DI, Lantos PL, eds. *Greenfield's Neuropathology*, Vol. 2, 7th edn. London: Hodder Arnold, 2002; 273–324.
15. Iwasaki Y, Yoshida M, Hashizume Y, Kitamoto T, Sobue G. Neuropathologic characteristics of spinal cord lesions in sporadic Creutzfeldt-Jakob disease. *Acta Neuropathol (Berl)* 2005; **110**: 490–500.
16. Iwasaki Y, Iijima M, Kimura S *et al.* Autopsy case of sporadic Creutzfeldt-Jakob disease presenting with signs suggestive of brainstem and spinal cord involvement. *Neuropathology* 2006; **26**: 550–556.
17. Iwasaki Y, Yoshida M, Hashizume Y, Kitamoto T, Sobue G. Pyramidal tract degeneration in sporadic Creutzfeldt-Jakob disease. *Neuropathology* 2007; **27**: 434–441.
18. Collinge J, Sidle KC, Meads J, Ironside J, Hill AF. Molecular analysis of prion strain variation and the aetiology of 'new variant' CJD. *Nature* 1996; **383**: 685–690.
19. Zanusso G, Farinazzo A, Fiorini M *et al.* pH-dependent prion protein conformation in classical Creutzfeldt-Jakob disease. *J Biol Chem* 2001; **276**: 40377–40380.
20. Cali I, Castellani R, Yuan J *et al.* Classification of sporadic Creutzfeldt-Jakob disease revisited. *Brain* 2006; **129**: 2266–2277.

Biochemical and Biophysical Research Communications 369 (2008) 1195–1198

Contents lists available at ScienceDirect

Biochemical and Biophysical Research Communications

journal homepage: www.elsevier.com/locate/ybbrc

Thr but Asn of the *N*-glycosylation sites of PrP is indispensable for its misfolding

Shino Ikeda, Atsushi Kobayashi, Tetsuyuki Kitamoto *

Division of CJD Science and Technology, Department of Prion Research, Tohoku University Graduate School of Medicine, 2-1 Seiryo-machi, Aoba-ku, Sendai 980-8575, Japan

ARTICLE INFO

Article history:
Received 27 February 2008
Available online 14 March 2008

Keywords:
Prion protein
N-linked glycosylation
Conversion
Site-directed mutagenesis

ABSTRACT

Prion protein (PrP) contains two *N*-linked glycosylation sites. It is unknown which amino acid substitution contributes most efficiently to the abolishment of *N*-linked glycosylations. To define the influence of amino acid substitution at the *N*-linked glycosylation sites on the conversion efficiency of mouse PrP, we tested each of all 19 amino acid substitutions at either one of the *N*-linked glycosylation sites (codon 180, 182, 196 or 198). The conversion efficiency of the mutagenized PrP was highly dependent on the newly introduced amino acid itself regardless of the absence of *N*-linked glycosylation in scrapie-infected mouse neuroblastoma cells. The majority of mutant PrP with substitutions at the Asn residues of the *N*-linked glycosylation sites were conversion-competent, whereas most mutant PrP with substitutions at the Thr residues were conversion-incompetent. These findings emphasize that the Asn residues of the *N*-linked glycosylation sites are replaceable to abolish *N*-linked glycosylations without directly affecting the protein function.

Prion diseases are lethal transmissible neurodegenerative disorders including Creutzfeldt–Jakob disease (CJD) in human, scrapie in sheep, and bovine spongiform encephalopathy in cattle. A central event in prion diseases appears to be a conformational conversion of the cellular isoform of prion protein (PrP^{C}) into an abnormal isoform (PrP^{Sc}) [1].

Prion protein (PrP) contains two *N*-linked glycosylation sites at codon 180 (N180) and codon 196 (N196) in mice (The consensus sequence is N-*X*-S/T). These *N*-linked glycosylation sites are highly conserved among mammalian species [2]. Two *N*-linked glycosylation sites are variably glycosylated, and the ratio of un-, mono- and di-glycosylated PrP varies among brain regions or animal species [3,4]. Moreover, the size of the protease resistant core of PrP^{Sc} (PrP^{res}) and the ratio of the three PrP^{res} glycoforms are characteristic markers of prion strains [4–6]. These facts lead us to suppose that the *N*-linked glycosylations may play an important role in the physiological function of PrP^{C} or prion replication. Meanwhile, several reports have demonstrated that the *N*-linked glycosylations are not essential for the PrP conversion process. (i) a point mutation at the first *N*-linked glycosylation site of human PrP (T183A, corresponding to T182A in mouse PrP) causes genetic CJD [7,8], (ii) transgenic mice expressing mouse PrP with an amino acid substitution at either one of the *N*-linked glycosylation sites developed disease when inoculated with scrapie prions [9,10], (iii) PrP^{C} in which either one or both of the *N*-linked glycosylations were disrupted by amino acid substitution at the *N*-linked glycosylation sites or by tunicamycin treatment converted into PrP^{res} in scrapie-infected mouse neuroblastoma (ScN2a) cells [9,11,12]. In these studies, however, the introduced mutations and altered residues of the *N*-linked glycosylation sites varied among the experiments. Similarly in many proteins, various amino acid substitutions have been utilized to abolish *N*-linked glycosylations without a theoretical background. Thus, it remains unclear which amino acid substitution is the most suitable without a direct effect on the (patho)physiological functions of the glycoprotein.

To investigate the influence of amino acid substitution at the *N*-linked glycosylation sites on the conversion efficiency of mouse PrP, we systematically introduced 19 amino acid substitutions at either one of the glycosylation sites (N180, T182, N196 or T198). The conversion efficiency of the mutant PrP highly depended on the substituted amino acid itself irrespective of the lack of *N*-linked glycosylation. Here we report the advantage of systematic amino acid substitution at the Asn residues of the *N*-linked gycosylation sites.

Materials and methods

Cell culture. ScN2a cells were kindly provided by Dr. Stanley B Prusiner [13]. ScN2a cells were cultured in Dulbecco's modified Eagle's medium (Invitrogen) containing 10% fetal bovine serum, 100 units/ml penicillin, and 100 μg/ml streptomycin at 37 °C in 5% CO_2.

* Corresponding author. Fax: +81 22 717 8148.
E-mail address: kitamoto@mail.tains.tohoku.ac.jp (T. Kitamoto).

0006-291X/$ - see front matter © 2008 Elsevier Inc. All rights reserved.
doi:10.1016/j.bbrc.2008.03.014

Plasmid construction. The open reading frame of mouse PrP was amplified by PCR with mouse DNA. The amplified fragment was cloned into pBluescript plasmid (Stratagene). The epitope for the monoclonal antibody 3F4 (L108M and V111M [14]) and amino acid substitutions at codon 180, 182, 196 or 198 were introduced into mouse PrP by site-directed PCR mutagenesis (Stratagene) according to the manufacturer's instructions. Introduction of the 3F4 epitope allows detection of transfected recombinant PrP against endogenous mouse PrP. After digestion with BamHI and XhoI, these 3F4 epitope-tagged mutant PrP fragments were cloned into the expression vector pSPOX [15]. The sequence of each mutant PrP construct was confirmed by sequencing analysis using the ABI PRISM 3100 genetic analyzer (Applied Biosystems).

Transfection and Western blotting. ScN2a cells were transiently transfected with plasmid constructs (6 μg DNA per 10 cm dish) using the FuGENE 6 transfection reagent (Roche Diagnostics). The medium was exchanged after 12 h of transfection. After 48 h of transfection, the cells were washed with PBS and harvested with 1 ml of lysis buffer (100 mM NaCl, 10 mM Tris–HCl pH 7.5, 1 mM EDTA, 0.5% Triton X-100, and 0.5% sodium deoxycholate), and the cell debris and nuclei were removed by low-speed centrifugation. For the detection of PrP^{res}, the cell lysates were digested with 20 μg/ml proteinase K (PK) at 37 °C for 30 min in the presence of 2% sarkosyl, and then the digestion was stopped by adding 2 mM of Pefabloc SC (Roche Diagnostics). The digested samples were ultracentrifuged at 100,000g, 20 °C for 1 h, and the pellets were resuspended with sample buffer (2% SDS, 60 mM Tris–HCl pH 6.8, 5% β-mercaptoethanol, 5% glycerol, and 0.01% bromophenol blue) and boiled. To compare the expression level and the glycosylation pattern of PrP, the undigested cell lysates were treated with sample buffer and boiled. For the deglycosylation of PrP, these samples were digested with 1500 units/ml PNGaseF (New England Biolabs) at 37 °C for 2 h. These samples were subjected to 13% SDS–PAGE and Western blotting as described [16]. The 3F4 monoclonal antibody (Signet Laboratories) was used as the primary antibody. Goat anti-mouse immunoglobulins polyclonal antibody labeled with the peroxidase-conjugated dextran polymer, EnVision+ (DakoCytomation) was used as the secondary antibody. Signals were visualized with an ECL Plus detection system (GE Healthcare Bio-Sciences). The signal intensities of Western blotting were quantified with Quantity One software using an imaging device VersaDoc 5000™ (Bio-Rad Laboratories). All experiments were repeated independently at least three times, and the representative data are shown.

Results and discussion

Amino acid substitution at the first N-linked glycosylation site (N180-I181-T182)

To investigate the influence of amino acid substitution at the first *N*-linked glycosylation site (N180 or T182), we systematically introduced an amino acid substitution into 3F4 epitope-tagged mouse PrP. We designated these mutant PrP as N180X or T182X (X is every possible amino acid). Western blot analysis of ScN2a cells transfected with these mutant PrP showed that all mutant PrP lacked the diglycosylated form except for T182S, which retained the *N*-linked glycosylation site (180N-I-182S) (Fig. 1A and F). The N180X mutant PrP was expressed almost equally (Fig. 1B and D). The T182X mutant PrP showed various expression levels (Fig. 1G and I). Only T182N and T182S were expressed moderately. After PK-digestion, most of N180X mutant PrP formed mono- and unglycosylated PrP^{res} (Fig. 1C and E). N180I, N180P and N180V formed a trace amount of PrP^{res}. In contrast, the T182X mutant PrP did not convert into PrP^{res} except for T182N and T182S (Fig. 1H and K). T182N formed only monoglycosylated PrP^{res}, while T182S formed monoglycosylated PrP^{res}, a trace of unglycosylated PrP^{res} and a smear of diglycosylated PrP^{res}.

Amino acid substitution at the second N-linked glycosylation site (N196-F197-T198)

Western blot analysis of ScN2a cells transfected with N196X or T198X mutant PrP showed that all mutant PrP lacked the

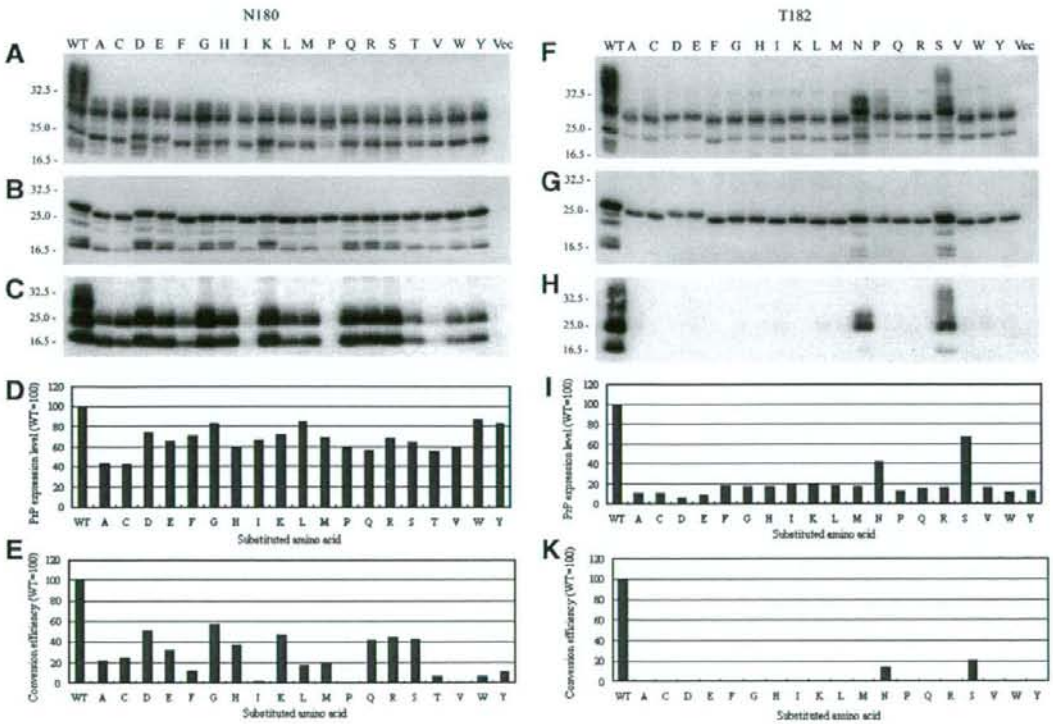

Fig. 1. Amino acid substitution at the first *N*-linked glycosylation site (N180 or T182). (A,F) Western blot analysis of ScN2a cells transfected with 3F4 epitope-tagged mutant PrP showed that mutant PrP lacked the diglycosylated form except for T182S. (B,G) The expression level of full-length mutant PrP was compared after deglycosylation with PNGaseF. (C,H) ScN2a cell lysates were digested with 20 μg/ml PK at 37 °C for 30 min. (D,I) The expression level of full-length mutant PrP was quantified. (E,K) The conversion efficiency of mutant PrP was quantified. WT: 3F4 epitope-tagged wild type PrP. Vec: pSPOX vector.

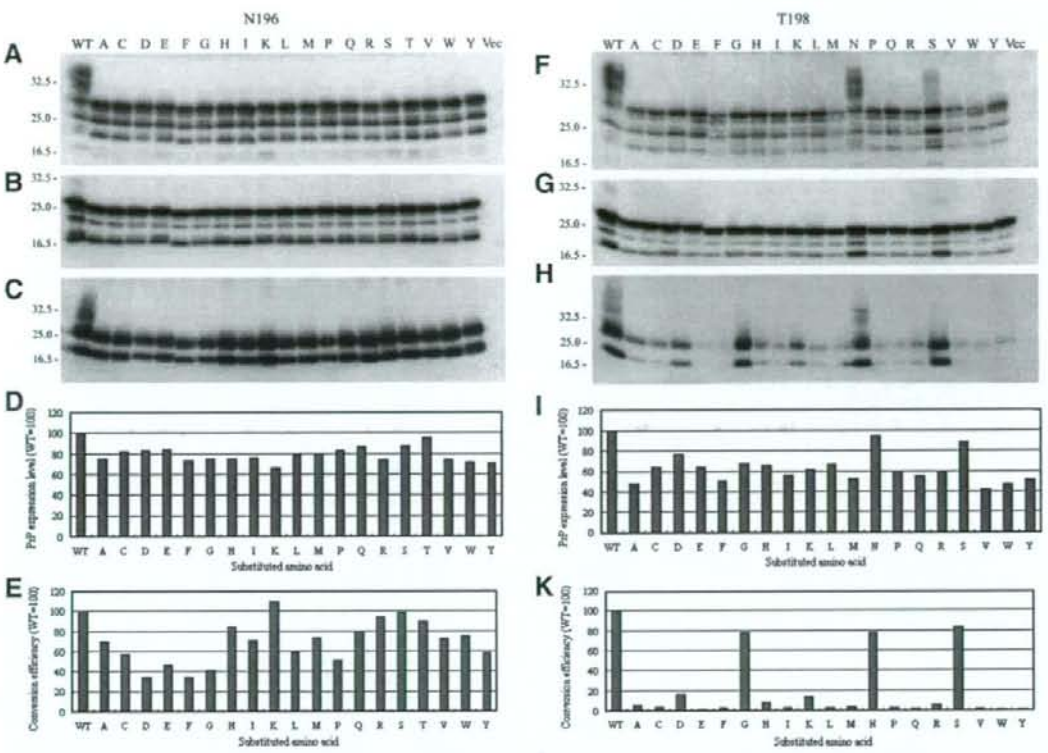

Fig. 2. Amino acid substitution at the second *N*-linked glycosylation site (N196 or T198). (A,F) Western blot analysis of ScN2a cells transfected with 3F4 epitope-tagged mutant PrP showed that mutant PrP lacked the diglycosylated form except for T198N and T198S. (B,G) The expression level of full-length mutant PrP was compared after deglycosylation with PNGaseF. (C,H) ScN2a cell lysates were digested with 20 μg/ml PK at 37 °C for 30 min. (D,I) The expression level of full-length mutant PrP was quantified. (E,K) The conversion efficiency of mutant PrP was quantified. WT: 3F4 epitope-tagged wild type PrP. Vec: pSPOX vector.

diglycosylated form except for T198N and T198S (Fig. 2A and F). T198S retained the *N*-linked glycosylation site (196N-F-198S), and T198N created a new glycosylation site (198N-E-200T). The expression level of N196X and T198X mutant PrP was almost equal to that of wild-type PrP (Fig. 2B,D,G and I). After PK-digestion, all N196X mutant PrP formed mono- and unglycosylated PrP^{res} (Fig. 2C and E). In contrast, T198X mutant PrP showed various conversion efficiencies (Fig. 2H and K). T198G, T198N and T198S were converted into PrP^{res} as well as wild-type PrP. T198A, T198C, T198D, T198H, T198I, T198K, T198L and T198R showed modest PrP^{res} formation. T198E, T198F, T198M, T198P, T198Q, T198V, T198W and T198Y formed a trace amount of PrP^{res}.

The present study demonstrated that mutant PrP lacking either one of the *N*-linked glycosylations is converted into PrP^{res} in ScN2a cells, and that the conversion efficiency of mutant PrP highly depends on the substituted amino acid. These findings agree with a report describing that the *N*-linked glycosylations are not required for PrP^{Sc} formation [9–12,17]. However, several mutations at codon 180, 182 or 198 prevented the PrP^{res} formation in the present study. These results suggest that the PrP conversion efficiency is altered by the amino acid substitution itself rather than the lack of *N*-linked glycosylation.

The reduction of the conversion efficiency of mutant PrP might be related to aberrant intracellular trafficking. In T182X mutant PrP, only T182N and T182S were expressed on the cell surface [9]. Although the subcellular localization of mutant PrP was not examined in this study, the conversion-incompetent mutations might cause protein instability, misfolding and aberrant trafficking of PrP.

The present study showed that the Asn residues of the *N*-linked glycosylation sites are more modifiable than the Ser/Thr residues. The majority of N180X or N196X mutant PrP was conversion-competent, whereas most of T182X and T198X mutant PrP was conversion-incompetent (Table 1). Both N180 and N196 are exposed to the surface of PrP, and large heterogeneous glycans are attached to these Asn residues [18]. Therefore, there might be enough space to accommodate any kind of side chain of the substituted amino

Table 1
Summary of the conversion efficiency of mutant PrP

	N180X	T182X	N196X	T198X
Lack of N-linked glycosylation[a]	19/19	18/19	19/19	17/19
Conversion competence[b]	11/19	1/19[c] (0/18)	19/19	3/19[d] (1/17)

[a] The number of mutant PrP lacking one *N*-linked glycosylation/the number of examined mutant PrP.

[b] The number of conversion-competent (conversion efficiency >20%) mutant PrP/the number of examined mutant PrP.

[c] T182S retained the *N*-linked glycosylation site. Therefore, the conversion competence of mutant PrP lacking an *N*-linked glycosylation is 0/18.

[d] T198S retained the *N*-linked glycosylation site, and T198N created a new *N*-linked glycosylation site. Therefore, the conversion competence of mutant PrP lacking an *N*-linked glycosylation is 1/17.

Table 2
Summary of the popular amino acid substitution at the *N*-linked glycosylation sites[b]

Altered residues	No. of reports	Substituted amino acids
Asn	49	Gln(31/49), Ala(12/49)
Ser/Thr	3	Gln(1/3), Ala(1/3), Ile(1/3)
Asn or Ser/Thr[a]	9	Asn→Gln (5/9), Ala(3/9) Ser/Thr→Ala(7/9), Gln(1/9)

[a] The Asn or Ser/Thr residue was altered respectively in an single *N*-linked glycosylation site.

[b] Cited papers: J. Biol. Chem. (2007) Dec 5 [J. Meng et al.: in press]; J. Virol. 82 (2008) 638–651; Mol. Cell. Endocrinol. 2007 Nov 2 [C. Stengel et al.: in press]; J. Cell. Biochem. 2007 Nov 2 [H. Zhao et al.: in press]; Am. J. Physiol. Gastrointest. Liver Physiol. 292 (2007) G818–G828; J. Biol. Chem. 282 (2007) 31733–31743; J. Virol. 81 (2007) 12029–12039; Acta. Biochim. Pol. 54 (2007) 567–573; Vaccine 25 (2007) 6572–6580; J. Lipid Res. 48 (2007) 2047–2057; Traffic 8 (2007) 431–444; Biochem. Biophys. Res. Commun. 356 (2007) 816–821; FEBS J. 274 (2007) 1202–1211; Biochemistry 46 (2007) 6617–6627; Virology 366 (2007) 415–423; Proc. Natl. Acad. Sci. USA 104 (2007) 10691–10696; J. Lipid Res. 48 (2007) 1132–1139; FEMS Yeast Res. 7 (2007) 1317–1327; J. Neurochem. 96 (2006) 843–852; Glycobiology 16 (2006) 258–270; Biosci. Biotechnol. Biochem. 70 (2006) 2476–2480; Insect Biochem. Mol. Biol. 36 (2006) 435–441; J. Biol. Chem. 281 (2006) 37353–37360; Infect. Immun. 73 (2005) 4478–4487; Biochem. J. 390 (2005) 105–113; J. Lipid Res. 45 (2004) 2080–2087; J. Bacteriol. 186 (2004) 6508–6514; Thromb. Haemost. 93 (2005) 1082–1088; J. Biol. Chem. 279 (2004) 21012–21020; Biochem. Pharmacol. 68 (2004) 1787–1796; FEBS Lett. 576 (2004) 21–26; Protein Sci. 13 (2004) 145–154; J. Biol. Chem. 279 (2004) 35320–35325; Biochem. J. 369 (2003) 179–184; Am. J. Physiol. Renal. Physiol. 284 (2003) F1199–F1206; Arch. Biochem. Biophys. 411 (2003) 19–26; Protein Expr. Purif. 26 (2002) 42–49; Thromb. Res. 105 (2002) 95–102; J. Lipid Res. 43 (2002) 1496–1507; Mol. Med. 8 (2002) 462–474; Biochem. J. 368 (2002) 495–505; J. Biol. Chem. 277 (2002) 43327–43334; J. Biol. Chem. 277 (2002) 50457–50462; Biochem. Biophys. Res. Commun. 297 (2002) 565–572; BMC Neurosci. (2002) 3:4; Biochem. Biophys. Res. Commun. 280 (2001) 1251–1257; J. Biol. Chem. 276 (2001) 576–582; Protein Eng. 14 (2001) 135–140; Biochemistry 40 (2001) 5392–5398; Biochem. J. 357 (2001) 73–81; Virus Res. 81 (2001) 151–156; Hum. Immunol. 61 (2000) 1202–1218; Glycobiology 10 (2000) 931–939; Thromb. Res. 99 (2000) 407–415; Protein Sci. 9 (2000) 985–990; Blood 95 (2000) 3357–3362; Biochemistry 39 (2000) 6514–6520; J. Pharmacol. Exp. Ther. 295 (2000) 404–409; J. Biochem. 127 (2000) 65–72; FEBS Lett. 467 (2000) 31–36; Biochemistry 39 (2000) 10189–10195.

acids at the Asn residues. Recently, it was reported that N196C mutant PrP in which the cysteine is labeled with the fluorescent dye acrylodan forms amyloid fibrils [19]. Thus, the Asn residues of the *N*-linked glycosylation sites could be modified with the side chains or with the fluorescent dye.

To date, many experiments have utilized a site-directed mutagenesis technique to abolish *N*-linked glycosylations in various proteins. In the 61 reports published during 2000-2008, the most popular substitution at the *N*-linked glycosylation sites is Asn→Gln (Table 2). Indeed, both N180Q and N196Q mutant PrP lacked the *N*-linked glycosylations without affecting the conversion competence in the present study. Moreover, our results show that the Asn residues of the *N*-linked glycosylation sites, rather than the Thr residue, are modifiable. Thus, in order to investigate the role of the *N*-linked glycosylation, we recommend that, at first, the amino acid substitution should be introduced at the Asn residues of the *N*-linked glycosylation sites. If all these mutant proteins lose their function, then the substitution at the Ser/Thr residues should be introduced as the next approach. If all mutant proteins lose their function in both approaches, it may be possible that *N*-linked glycosylation is essential for the function of the glycoprotein. Therefore, we conclude that the *N*-linked glycosylations are not essential for the PrP conversion process.

Acknowledgments

This study was supported by the Program for Promotion of Fundamental Studies in Health Sciences of National Institute of Biomedical Innovation (T.K.), a grant from the Ministry of Health, Labor and Welfare (A.K. and T.K.), and a Grant-in-Aid for Scientific Research from the Ministry of Education, Culture, Sports, Science and Technology (A.K. and T.K.). In addition, we thank R.-W. Shin, M. Morita and B. Bell for critical review of the manuscript.

References

[1] S.B. Prusiner, Prions, Proc. Natl. Acad. Sci. USA 95 (1998) 13363–13383.
[2] T. van Rheede, M.M. Smolenaars, O. Madsen, W.W. de Jong, Molecular evolution of the mammalian prion protein, Mol. Biol. Evol. 20 (2003) 111–121.
[3] S.J. DeArmond, Y. Qiu, H. Sánchez, P.R. Spilman, A. Ninchak-Casey, D. Alonso, V. Daggett, PrP^{Sc} glycoform heterogeneity as a function of brain region: implications for selective targeting of neurons by prion strains, J. Neuropathol. Exp. Neurol. 58 (1999) 1000–1009.
[4] R.A. Somerville, Host and transmissible spongiform encephalopathy agent strain control glycosylation of PrP, J. Gen. Virol. 80 (1999) 1865–1872.
[5] P. Parchi, S. Capellari, S.G. Chen, R.B. Petersen, P. Gambetti, N. Kopp, P. Brown, T. Kitamoto, J. Tateishi, A. Giese, H. Kretzschmar, Typing prion isoforms, Nature 386 (1997) 232–234.
[6] P. Parchi, A. Giese, S. Capellari, P. Brown, W. Schulz-Schaeffer, O. Windl, I. Zerr, H. Budka, N. Kopp, P. Piccardo, S. Poser, A. Rojiani, N. Streichemberger, J. Julien, C. Vital, B. Ghetti, P. Gambetti, H. Kretzschmar, Classification of sporadic Creutzfeldt–Jakob disease based on molecular and phenotypic analysis of 300 subjects, Ann. Neurol. 46 (1999) 224–233.
[7] R. Nitrini, S. Rosemberg, M.R. Passos-Bueno, L.S. da Silva, P. Iughetti, M. Papadopoulos, P.M. Carrilho, P. Caramelli, S. Albrecht, M. Zatz, A. LeBlanc, Familial spongiform encephalopathy associated with a novel prion protein gene mutation, Ann. Neurol. 42 (1997) 138–146.
[8] E. Grasbon-Frodl, H. Lorenz, U. Mann, R.M. Nitsch, O. Windl, H.A. Kretzschmar, Loss of glycosylation associated with the T183A mutation in human prion disease, Acta Neuropathol. 108 (2004) 476–484.
[9] E. Neuendorf, A. Weber, A. Saalmueller, H. Schatzl, K. Reifenberg, E. Pfaff, M.H. Groschup, Glycosylation deficiency at either one of the two glycan attachment sites of cellular prion protein preserves susceptibility to bovine spongiform encephalopathy and scrapie infections, J. Biol. Chem. 279 (2004) 53306–53316.
[10] F. Wiseman, E. Cancellotti, J. Manson, Glycosylation and misfolding of PrP, Biochem. Soc. Trans. 33 (2005) 1094–1095.
[11] A. Taraboulos, M. Rogers, D.R. Borchelt, M.P. McKinley, M. Scott, D. Serban, S.B. Prusiner, Acquisition of protease resistance by prion proteins in scrapie-infected cells does not require asparagine-linked glycosylation, Proc. Natl. Acad. Sci. USA 87 (1990) 8262–8266.
[12] C. Korth, K. Kaneko, S.B. Prusiner, Expression of unglycosylated mutated prion protein facilitates PrP^{Sc} formation in neuroblastoma cells infected with different prion strains, J. Gen. Virol. 81 (2000) 2555–2563.
[13] D.A. Butler, M.R. Scott, J.M. Bockman, D.R. Borchelt, A. Taraboulos, K.K. Hsiao, D.T. Kingsbury, S.B. Prusiner, Scrapie-infected murine neuroblastoma cells produce protease-resistant prion proteins, J. Virol. 62 (1988) 1558–1564.
[14] R.J. Kascsak, R. Rubenstein, P.A. Merz, M. Tonna-DeMasi, R. Fersko, R.I. Carp, H.M. Wisniewski, H. Diringer, Mouse polyclonal and monoclonal antibody to scrapie-associated fibril proteins, J. Virol. 61 (1987) 3688–3693.
[15] M.R. Scott, R. Kohler, D. Foster, S.B. Prusiner, Chimeric prion protein expression in cultured cells and transgenic mice, Protein Sci. 1 (1992) 986–997.
[16] M. Asano, S. Mohri, J.W. Ironside, M. Ito, N. Tamaoki, T. Kitamoto, vCJD prion acquires altered virulence through trans-species infection, Biochem. Biophys. Res. Commun. 342 (2006) 293–299.
[17] S.J. DeArmond, H. Sánchez, F. Yehiely, Y. Qiu, A. Ninchak-Casey, V. Daggett, A.P. Camerino, J. Cayetano, M. Rogers, D. Groth, M. Torchia, P. Tremblay, M.R. Scott, F.E. Cohen, S.B. Prusiner, Selective neuronal targeting in prion disease, Neuron 19 (1997) 1337–1348.
[18] E. Stimson, J. Hope, A. Chong, A.L. Burlingame, Site-specific characterization of the *N*-linked glycans of murine prion protein by high-performance liquid chromatography/electrospray mass spectrometry and exoglycosidase digestions, Biochemistry 38 (1999) 4885–4895.
[19] Y. Sun, L. Breydo, N. Makarava, Q. Yang, O.V. Bocharova, I.V. Baskakov, Site-specific conformational studies of prion protein (PrP) amyloid fibrils revealed two cooperative folding domains within amyloid structure, J. Biol. Chem. 282 (2007) 9090–9097.

Neuropathology 2008; **28**, 645–651 doi:10.1111/j.1440-1789.2008.00904.x

Case Report

MM2-cortical-type sporadic Creutzfeldt-Jakob disease with early stage cerebral cortical pathology presenting with a rapidly progressive clinical course

Yoshiki Niimi,[1] Yasushi Iwasaki,[1] Toshitaka Umemura,[2] Fumiaki Tanaka,[1] Mari Yoshida,[3] Yoshio Hashizume,[3] Tetsuyuki Kitamoto,[4] Mikio Hirayama[2] and Gen Sobue[1]

[1]Department of Neurology, Nagoya University Graduate School of Medicine, Nagoya, [2]Department of Neurology, Kasugai Municipal Hospital, Kasugai, [3]Department of Neuropathology, Institute for Medical Science of Aging, Aichi Medical University, Aichi, and [4]Division of CJD Science and Technology, Department of Prion Research, Center for Translational and Advanced Animal Research on Human Diseases, Tohoku University Graduate School of Medicine, Sendai, Japan

We report the case of a 67-year-old man with MM2-cortical-type sporadic Creutzfeldt-Jakob disease (sCJD) with a rapidly progressive clinical course of 5 months. Initial symptoms were progressive memory disturbance and dementia. MRI revealed high signal-intensity lesions on diffusion-weighted images in the bilateral frontal and occipital cortices. Myoclonus and periodic sharp-wave complexes on the electroencephalogram were observed in the early disease stage. The clinical diagnosis was typical sCJD. Neuropathologic examination at autopsy showed widespread, characteristic cerebral neocortical involvement with large confluent vacuole-type spongiform change. Spongiform degeneration was also evident in the striatum and medial thalamus. In the cerebellar cortex, slight depletion of Purkinje neurons was evident without spongiform change in the molecular layer or apparent neuron loss in the granule cell layer. The inferior olivary nucleus showed slight hypertrophic astrocytosis without neuron loss. Prion protein (PrP) immunostaining showed widespread, characteristic perivacuolar-type PrP deposits with irregular plaque-like PrP deposits in the cerebral neocortex, striatum and medial thalamus. We believe this patient showed early-stage cerebral cortical pathology of MM2-cortical-type sCJD, which may provide clues regarding the pathologic progression of this rare sCJD subtype. Although MM2-cortical-type sCJD generally shows slow progression without myoclonus or periodic sharp-wave complexes, the present patient showed a rapidly progressive clinical course similar to that of MM1-type sCJD.

Key words: irregular plaque-like prion protein deposition, large confluent vacuole-type spongiform change, MM2-cortical-type, perivacuolar-type prion protein deposition, sporadic Creutzfeldt-Jakob disease.

INTRODUCTION

The clinicopathologic presentation of sporadic Creutzfeldt-Jakob disease (sCJD) is influenced by several factors including the prion strain and polymorphism of the prion protein (PrP) gene of the host.[1–3] Analyses of the neuropathologic findings as well as clinical features will lead to a better understanding of such factors.[1–3] sCJD has been classified according to the genotype of methionine (M)/valine (V) polymorphism at codon 129 of the PrP gene and the physicochemical properties of PrP of type 1/type 2.[2,4] A simple classification system proposed by Parchi *et al.*[2] has been widely accepted and recognizes six phenotypes of sCJD: MM1, MM2, MV1, MV2, VV1 and VV2. MM2-type sCJD is further divided into two distinct phenotypes: MM2-cortical-type, which shows features of slowly progressive dementia without other neurologic abnormalities, and MM2-thalamic-type, which shows striking similarities to features of fatal familial insomnia.[2,3] Although such

Correspondence: Yasushi Iwasaki, MD, Department of Neurology, Nagoya University Graduate School of Medicine, 65 Tsurumai-cho, Showa-ku, Nagoya 466-8550, Japan. Email: iwasaki@sc4.so-net.ne.jp

Received 31 July 2007; revised 17 December 2007; accepted 20 January 2008.

classification systems are helpful in the identification and understanding of major sCJD subgroups, there remain individual cases that prove difficult to classify on this basis.[1,5] MM2-cortical-type sCJD was not recognized prior to 1999,[2] although the type of spongiform degeneration that characterizes this subtype was reported in earlier studies.[6,7] MM2-cortical-type sCJD is found in only 2%–8% of patients with sCJD,[2,3,8] and there have been few detailed neuropathologic investigations of this type.[9] The possibility of a higher prevalence of MM2-cortical-type sCJD than has been assumed cannot be excluded because some patients with MM2-cortical-type sCJD may be misdiagnosed.[8] Prolonged disease duration, late occurrence of typical CJD symptoms other than dementia and the low sensitivity of electroencephalography (EEG) make the diagnosis of MM2-cortical-type sCJD difficult.[2,8,10] Because of the nonspecific symptoms,[8,10,11] Alzheimer disease (AD) and dementia with Lewy bodies are considered important differential diagnoses.[10] Thus, further detailed clinicopathologic investigations of MM2-cortical-type sCJD are needed.

We report the case of a patient with MM2-cortical-type sCJD who presented with rapidly progressive dementia with myoclonus and periodic sharp-wave complexes (PSWCs) on EEG. The patient died 5 months after symptom onset. We discuss the clinicopathologic aspects of this case with respect to sCJD phenotypic variability.

CLINICAL SUMMARY

A 67-year-old Japanese man, who lived in the Aichi prefecture of the Tokai district, Japan, began to experience memory disturbances in June 2005. He had no history of surgery or blood transfusion or any family history of prion disease. Memory disturbances and dementia developed rapidly, and he was referred to the Department of Neurology at Kasugai Municipal Hospital in August 2005. Neurologic examination showed aphasia; decreased spontaneous speech and word-finding difficulty were observed. Only simple words were spoken. The patient was able to repeat a word, but word perseveration was observed. He was not able to answer questions regarding his name, age or town. Apraxia, including finger agnosia and right-left disorientation, was observed. Agnosia, including ideomotor apraxia, was also observed. Extrapyramidal signs, including rigidity of the extremities, nuchal rigidity, brachybasia and bradykinesia, were found. Pyramidal signs, including spasticity of the extremities were found, but tendon reflexes were normal, without Babinski's sign. Myoclonus was noted, particularly in the right leg. The CSF showed a mild increase in neuron-specific enolase (NSE) (22.4 ng/mL [normal <14 ng/mL]). CSF 14-3-3 protein was not examined. MRI revealed high signal-intensity lesions on diffusion-weighted images (DWI) in both the frontal and occipital cortices (Fig. 1a). Single-photon emission computed tomography (ECD-SPECT) showed a moderate reduction of cerebral blood flow bilaterally in the frontal, parietal and occipital lobes, with preserved cerebral blood flow in the basal ganglia and thalamus (Fig. 1b). EEG showed slow-wave activity with PSWCs (Fig. 1c). Typical sCJD was suspected according to these clinical findings. The patient rapidly entered an apathetic state with decreased speech and appetite. Dysphagia developed in September 2005, and rigospasticity in the extremities became exaggerated. The patient choked while eating and died of respiratory failure in November 2005 at the age of 68, 5 months after the onset of symptoms. A state of akinetic mutism was not observed until the patient was close to death.

METHODS

Neuropathologic examination

Autopsy was performed 15 h after death. The brain was fixed in 20% neutral-buffered formalin, and tissue blocks were immersed in 95% formic acid (Wako Pure Chemical Industries, Osaka, Japan) overnight to inactivate prion infectivity. The spinal cord was not available. Eight-micrometer-thick, paraffin-embedded sections were then prepared. For routine neuropathologic examination, sections were subjected to HE, KB and Congo red staining. Immunohistochemical analysis was carried out with monoclonal antibody 3F4 against PrP (1:100; Dako, Glostrup, Denmark) after hydrolytic autoclaving to retrieve antigen.[12] The PrP immunostaining protocol was as described previously.[13]

PrP gene analysis and Western blot analysis

Genomic DNA was extracted from cryopreserved brain and used to amplify the open reading frame of the PrP gene by PCR. We searched for PrP gene mutations and polymorphisms at codons 129 and 219 by restriction fragment length polymorphism analysis and by sequencing as described previously.[1]

Frozen right frontal cerebral cortex was homogenized, and Western blot analysis of protease-resistant PrP was performed with monoclonal antibody 3F4 as described previously.[1] Typing of PrP was performed on the basis of the classification system proposed by Parchi *et al.*[2,4]

PATHOLOGIC FINDINGS

Macroscopic findings

The gross appearance of the brain was normal, and it weighed 1385 g. On coronal sections, the cerebrum showed slight neocortical atrophy of the occipital lobe (Fig. 2a).

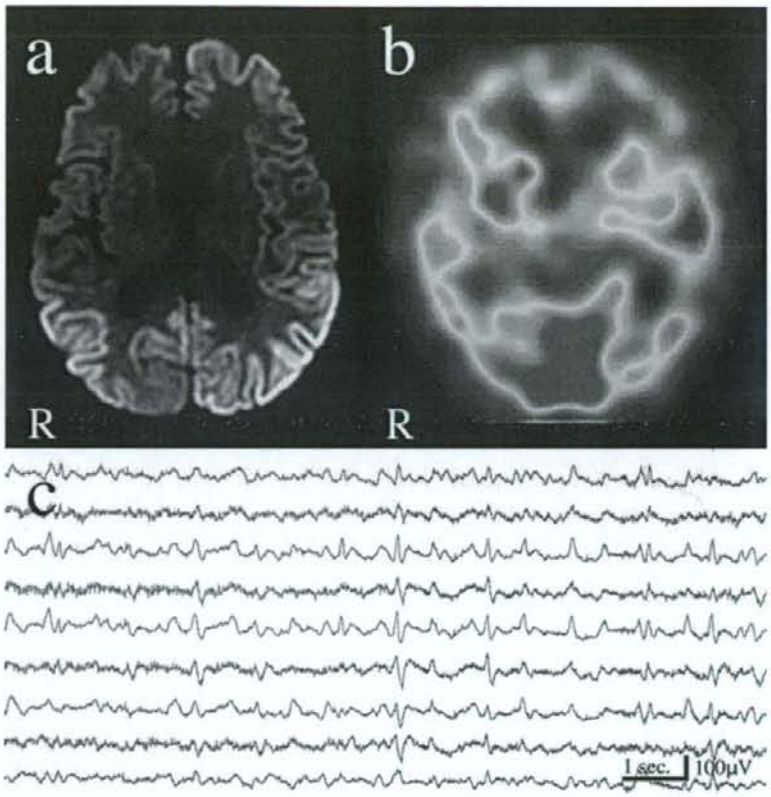

Fig. 1 Diagnostic images. (a) MRI obtained 2 months after the onset of symptoms shows high signal-intensity lesions on diffusion-weighted images bilaterally in the frontal and occipital cortices (more so in the left occipital cortex). Ventricular dilatation is also apparent. (b) ^{99m}Tc-ethyl cysteinate dimer single-photon emission CT scan obtained 3 months after the onset of symptoms shows moderate reduction of cerebral blood flow bilaterally in the frontal, parietal and occipital lobes (more so in the left parietal lobe). (c) Electroencephalogram obtained 3 months after the onset of symptoms shows slow-wave activity with periodic sharp-wave complexes. R, right side.

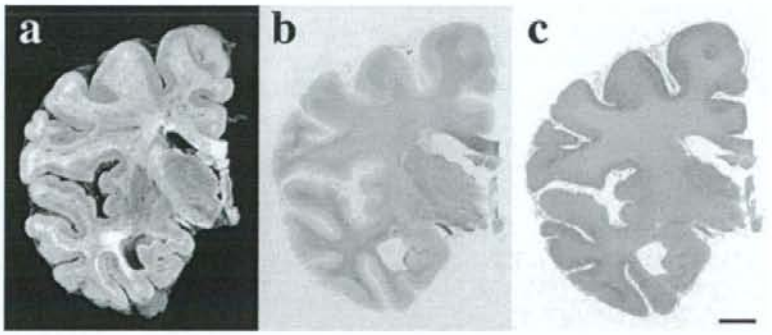

Fig. 2 Macroscopic images of coronal sections of the cerebral hemisphere. (a) Although no apparent neocortical atrophy is shown, slight neocortical atrophy is observed in the occipital lobe. The striatum, thalamus and hippocampus are well preserved. (b) The cerebral white matter shows no myelin pallor. KB staining. (c) Immunostaining for prion protein shows dot-like staining in the gray matter, particularly in the cerebral neocortex. Scale bar, 10 mm.

The basal ganglia, thalamus and cerebral white matter showed no abnormality. Ammon's horn was well preserved. No cerebellar or brainstem atrophy was apparent.

Microscopic findings

Routine pathologic evaluation of the organs revealed no abnormality such as infection, pneumonia, sepsis or organ failure.

In the cerebral cortex, widespread spongiform degeneration characterized by large confluent vacuole-type spongiform change (large vacuoles in small coalescing groups[1-3]) of varying severity was observed (Fig. 3a). Spongiform degeneration was moderate in the anterior region and orbital surface of the frontal lobe and in the temporal and occipital lobes, cingulate gyrus and insular cortex (Fig. 3b), mild in the posterior region of the frontal lobe, including the precentral gyrus, parahippocampal

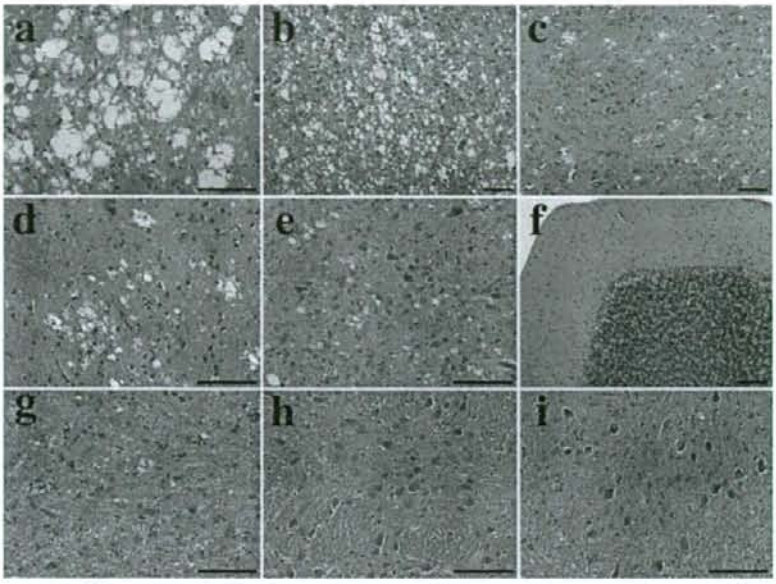

Fig. 3 Representative microscopic images of gray-matter lesions. (a) The cerebral neocortex shows widespread large confluent vacuole-type spongiform change with mild gliosis. Temporal lobe. (b) The occipital lobe shows moderate spongiform degeneration. Neurons are relatively preserved in number, and hypertrophic astrocytosis is generally mild. (c) The posterior region of the frontal lobe shows mild spongiform degeneration. Precentral gyrus. (d) The striatum shows some large confluent vacuole-type spongiform change with mild gliosis. Putamen. (e) The medial thalamus shows mild spongiform degeneration with moderate gliosis. (f) The molecular layer of the cerebellum shows no atrophy or spongiform degeneration, and the granule cell layer is well preserved from neuron loss, whereas the Purkinje neuron layer shows slight neuron loss with Bergmann gliosis and some torpedos. (g) The quadrigeminal body shows mild spongiform degeneration and neuron loss with moderate hypertrophic astrocytosis. (h) The pontine nucleus is preserved from neuron loss and gliosis. (i) The inferior olivary nucleus shows mild hypertrophic astrocytosis without apparent neuron loss. All panels, HE staining. Scale bars, 100 μm.

gyrus and parietal lobe (Fig. 3c), and sparse in the subiculum and amygdala. Status spongiosus (severe neuron loss with severe tissue rarefaction, hypertrophic astrocytosis and irregular cavities[1]) was not observed. In the cerebral neocortex, neurons were relatively preserved in number, and hypertrophic astrocytosis was generally mild (Fig. 3a–c). In the hippocampus, spongiform degeneration and gliosis were not observed. In the striatum and medial thalamus, mild spongiform degeneration, with relatively preserved neurons and mild gliosis, was evident (Fig. 3d,e). The lateral thalamus and pallidum were relatively preserved from spongiform degeneration and gliosis. Although the cerebral white matter was well preserved, without myelin pallor (Fig. 2b), some mild gliosis was observed in the temporal and occipital subcortices. In the cerebellar cortex, the molecular layer showed no atrophy or spongiform degeneration, and the granule cell layer was well preserved from neuron loss, whereas the Purkinje neuron layer showed slight neuron loss with Bergmann gliosis and torpedos (Fig. 3f). The dentate nucleus was well preserved without gliosis or grumose degeneration. The cerebellar white matter was well preserved without myelin pallor. Although the tegmentum of the brainstem showed no apparent atrophy, the quadrigeminal body showed mild spongiform degeneration and neuron loss with moderate hypertrophic astrocytosis (Fig. 3g). Neuron loss and gliosis was not apparent in the substantia nigra, pontine nucleus (Fig. 3h) or locus ceruleus. The inferior olivary nucleus showed mild hypertrophic astrocytosis without apparent neuron loss (Fig. 3i). Pyramidal tract degeneration was not observed. Florid plaques or kuru plaques were not observed. Senile plaques, neurofibrillary tangles or Lewy bodies were also not observed. No vascular lesions were observed. No congophilia was observed by Congo red staining.

PrP immunohistochemical findings

PrP immunostaining showed widespread PrP deposition characterized by perivacuolar-type deposits[1–3,14] (intense PrP deposits surrounding areas of confluent spongiform change) with spotted coarse and irregular plaque-like structures that were not identifiable by HE staining[1–3] (primitive plaque-type PrP deposition,[2,3] as also described in our previous report[1,5]) in the cerebral neocortex (Figs 2c and 4a,b). PrP immunoreactivity was most prominent in the occipital cortex, followed by the temporal cortex. Perivacuolar-type PrP deposition was predominant in the occipital and temporal cortices, whereas irregular plaque-like PrP deposition was predominant in the frontal and parietal cortices (Fig. 4a,b). In the striatum and medial thalamus, PrP deposition was mild and showed perivacuolar-type and irregular plaque-like PrP deposition (Fig. 4c). In the cerebellum, sparse irregular plaque-like PrP deposition was observed in the molecular layer, and mild synaptic-type PrP deposition (diffuse fine granular staining pattern[1–3,12,14]) was observed in the granule cell layer (Fig. 4d). The Purkinje neuron layer and dentate

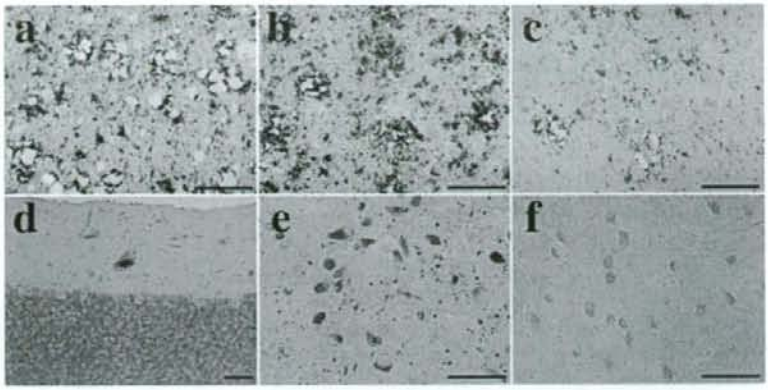

Fig. 4 Representative microscopic images of prion protein (PrP) immunostaining. (a) Perivacuolar-type PrP deposition is predominant in the temporal lobe. (b) Irregular plaque-like PrP deposition is predominant in the frontal lobe. (c) The striatum shows mild perivacuolar-type PrP deposition with some irregular plaque-like PrP deposition. Putamen. (d) The cerebellar cortex shows sparse irregular plaque-like PrP deposits in the molecular layer and mild synaptic-type PrP deposition in the granule cell layer. (e) The locus ceruleus shows many small kuru plaque-like PrP deposits. (f) The inferior olivary nucleus shows mild synaptic-type PrP deposition. Scale bars, 100 μm.

nucleus showed no PrP immunoreactivity. In the brainstem, the locus ceruleus showed many small kuru plaque-like PrP deposits (these small plaques were not identified by HE staining) (Fig. 4e). Mild synaptic-type PrP deposition was observed in the quadrigeminal body and inferior olivary nucleus (Fig. 4f). In the pontine nucleus, PrP deposition was sparse. PrP deposition was not observed in the cerebral, cerebellar or brainstem white matter.

PrP gene analysis and Western blot analysis

PrP gene analysis showed no mutation in the open reading frame and showed methionine homozygosity at codon 129. Codon 219 showed glutamic acid homozygosity. Western blot analysis showed type 2 PrP,[2,4] with the relative molecular mass of the non-glycosylated band being 19 kDa (Fig. 5).

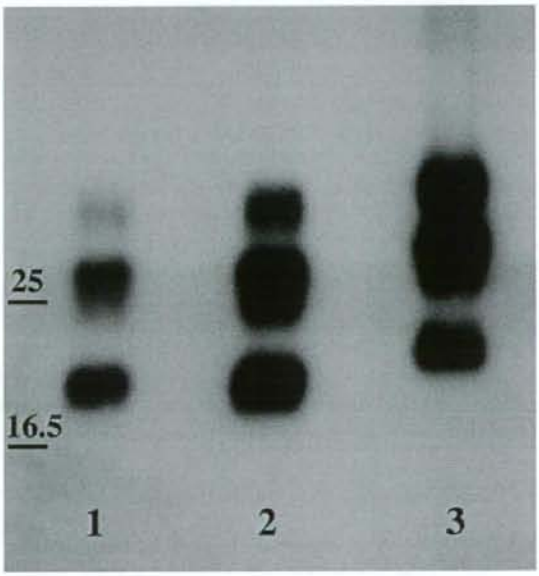

Fig. 5 Western blot analysis of prion protein (PrP). The gel mobility of PrP from frozen right frontal cerebral cortex of the present patient (lane 2) is compared with that of PrP from two patients with sporadic Creutzfeldt-Jakob disease (sCJD) (lane 1: MM2-type sCJD; lane 3: MM1-type sCJD). PrP migrated as three bands that have been shown to correspond to the diglycosylated (upper band), monoglycosylated (middle band) and non-glycosylated (lowest band) forms of the protein.

DISCUSSION

On the basis of the clinical findings of rapidly progressive dementia with myoclonus and PSWCs on EEG, sCJD was readily diagnosed in the early disease stage in the present case. Although typical sCJD was suspected clinically, PrP gene and Western blot analyses showed rare, atypical sCJD of the MM2-type. We believe this case should be classified as MM2-cortical-type sCJD for the following reasons: cerebral cortical hyperintensity was observed on DWI; cerebral blood flow in the thalamus, which is decreased in MM2-thalamic-type sCJD,[10] was preserved; widespread large confluent vacuole-type spongiform change and perivacuolar-type PrP deposition, which are characteristic of MM2-cortical-type sCJD,[2] were observed in the cerebral cortices; particular medial thalamic and inferior olivary degeneration, which are found in MM2-thalamic-type sCJD,[1,5] were not observed. On the basis of these findings, we believe the present case does not represent the combined thalamic form of sCJD, although the existence of this corticothalamic form of MM2-type sCJD should be noted.[10] We analyzed PrP type in only one frozen cerebral sample (right frontal cerebral cortex) in the present case. Thus, the possibility of the coexistence of type 1 and type 2 PrP in the present case cannot be ruled out. However, we believe this patient did not have MM1-type sCJD because